

Supporting Information

For

Axially Chiral Stable Radicals: Resolution and Characterization of Blatter Radical Atropisomers

Agnieszka Bodzioch,^{†*} Anna Pietrzak,[⊥] and Piotr Kaszyński^{†‡§*}

[†] Centre of Molecular and Macromolecular Studies, Polish Academy of Sciences, 90-363 Łódź, Poland
Faculty of Chemistry, Łódź University of Technology, Żeromskiego 116, 90-024, Łódź, Poland

[‡] Faculty of Chemistry, University of Łódź, 91-403 Łódź, Poland.

[§] Department of Chemistry, Middle Tennessee State University, Murfreesboro, TN, 37132, USA

	Page
1. Synthetic and characterization detailsS2
2. NMR spectraS6
3. IR spectraS10
4. XRD dataS11
5. UV-vis spectroscopyS14
6. EPR spectroscopyS15
7. Electrochemical resultsS17
8. Chiral HPLC analysis and resolutionS19
9. Optical rotationS21
10. Electronic circular dichroism spectroscopyS21
11. Determination of absolute configuration of the atropisomersS23
12. Kinetic analysis of racemizationS27
13. Computational detailsS34
14. Partial output from TD-DFT calculationsS34
15. Archive for DFT calculationsS40
16. ReferencesS44

1. Synthetic and characterization details

Reagents and solvents were obtained commercially.

Heat in reactions involving elevated temperatures was supplied using oil baths, and reported temperature refers to that of the bath.

NMR spectra were obtained at 400 (^1H) and 100 MHz (^{13}C) in CDCl_3 or $\text{DMSO}-d_6$. Chemical shifts were referenced to the solvent (^1H and ^{13}C : 7.26 and 77.16 ppm for CDCl_3 , and 2.50 and 39.52 ppm for $\text{DMSO}-d_6$, respectively).¹ Melting points were determined on a Melt-Temp II apparatus in capillaries, and they are uncorrected. The ESI-MS spectra were obtained using a Varian 500 MS LS Ion Trap spectrometer. IR spectra were measured in KBR pellets.

*Preparation of racemic radicals **rac-1**. A general procedure.*

A solution of an organolithium reagent (generated from 1.3 mmol of appropriate bromonaphthalene and 2.6 mmol *t*-BuLi) in THF (3 mL) was added dropwise at -78 °C to a stirred solution of corresponding benzo[*e*][1,2,4]triazine **2** (1.0 mmol) in dry THF (3 mL). The resulting mixture was stirred for 20 min at -78 °C and at rt for 30 min. Then it was opened to air and stirred overnight at rt. Water and CH_2Cl_2 were added and the organic phase was separated, washed with water and dried (Na_2SO_4). After evaporation of solvent the resulting crude product was purified by column chromatography (SiO_2 passivated with 1% Et_3N in hexane, hexane/AcOEt) to afford radicals **rac-1**. Analytically pure radicals were obtained by recrystallization from *n*-heptane.

3-Phenyl-1-(8-phenylnaphth-1-yl)-1,4-dihydrobenzo[*e*][1,2,4]triazin-4-yl (rac-1aA**).** Radical **rac-1aA** (161 mg, 0.392 mmol, 62% yield) was obtained from 3-phenylbenzo[*e*][1,2,4]triazine² (**2a**, 131 mg, 0.632 mmol) and 1-bromo-8-phenylnaphthalene (**3A**, 224 mg, 0.794 mmol) as a dark brown solid. Recrystallization from *n*-heptane gave the analytically pure microcrystalline product in 44% yield: mp 179–180 °C (*n*-heptane); IR ν 3047, 1484, 1391, 831, 770, 695 cm^{-1} ; UV-vis (CH_2Cl_2) λ_{max} (log ϵ) 231 (4.69), 270 (4.48), 370 (3.56), 487 (3.15), 543 (2.81) nm; ESI-MS, *m/z* 411 (100, [M + H]⁺); HRMS (ESI-TOF) *m/z* [M+H]⁺ calcd for $\text{C}_{29}\text{H}_{21}\text{N}_3$ 411.1735, found 411.1719. Anal. Calcd for $\text{C}_{29}\text{H}_{20}\text{N}_3$: C, 84.85; H, 4.91; N, 10.24. Found: C, 84.72; H, 4.82; N, 10.25. Chiral HPLC: $t_{\text{R}1} = 14.45$ min (+), $t_{\text{R}2} = 16.79$ min (-).

1-[8-(4-*tert*-Butylphenyl)naphth-1-yl]-3-phenyl-1,4-dihydrobenzo[*e*][1,2,4]triazin-4-yl (rac-1aB**).** Racemic radical **rac-1aB** (51.0 mg, 0.109 mmol, 29% yield) was obtained from 3-phenylbenzo[*e*][1,2,4]triazine² (**2a**, 78.0 mg, 0.377 mmol) and 1-bromo-8-(4-*tert*-butylphenyl)naphthalene (**3B**, 141 mg, 0.416 mmol) as a dark brown powder: mp 108–109 °C (*n*-

heptane); IR ν 3057, 2961, 1485, 1392, 834, 756, 696 cm^{-1} ; UV-vis (CH_2Cl_2) λ_{\max} (log ϵ) 229 (4.75), 269 (4.60), 373 (3.65), 444 (3.40), 490 (3.27) nm; ESI-MS, m/z 467 (100, $[\text{M}+\text{H}]^+$); HRMS (ESI-TOF) m/z $[\text{M}+\text{H}]^+$ calcd for $\text{C}_{33}\text{H}_{29}\text{N}_3$: 467.2361, found 467.2357. Anal. Calcd for $\text{C}_{33}\text{H}_{28}\text{N}_3$: C, 84.95; H, 6.05; N, 9.01. Found: C, 85.01; H, 5.99; N, 9.08. Chiral HPLC: $t_{\text{R}1} = 9.85$ min (+), $t_{\text{R}2} = 11.47$ min (-).

3-*tert*-Butyl-1-(8-phenylnaphth-1-yl)-1,4-dihydrobenzo[*e*][1,2,4]triazin-4-yl (rac-1bA). Radical **rac-1bA** (49.0 mg, 0.126, 45% yield) was obtained from 3-(*tert*-butyl)benzo[*e*][1,2,4]triazine (**2b**, 29.0 mg, 0.155 mmol) and 1-bromo-8-phenylnaphthalene (**3A**, 53.0 mg, 0.188 mmol) as a dark brown solid. Recrystallization from *n*-heptane gave the analytically pure microcrystalline product in 11% yield: mp 177–178 °C (*n*-heptane); IR ν 3058, 2954, 1481, 1400, 832, 770, 699 cm^{-1} ; UV-vis (CH_2Cl_2) λ_{\max} (log ϵ) 233 (4.69), 296 (3.96), 346 (3.60), 442 (3.33), 544 (2.90) nm; ESI-MS, m/z 391 (90, $[\text{M}+\text{H}]^+$), 390 (100, M^+); HRMS (ESI-TOF) m/z $[\text{M}+\text{H}]^+$ calcd for $\text{C}_{27}\text{H}_{25}\text{N}_3$ 391.2048, found 391.2032. Anal. Calcd for $\text{C}_{27}\text{H}_{24}\text{N}_3$: C, 83.04; H, 6.19; N, 10.76. Found: C, 83.02; H, 6.07; N, 10.82. Chiral HPLC: $t_{\text{R}1} = 11.55$ min (+), $t_{\text{R}2} = 12.77$ min (-).

3-(*tert*-Butyl)benzo[*e*][1,2,4]triazine (2b**).³** Following the method of Koutentis,⁴ *N'*-(2-nitrophenyl)pivalohydrazide (**5**, 1.15 g, 4.85 mmol) was dissolved in glacial acetic acid (40 mL), Sn powder (2.30 g, 19.4 mmol) was added, and the solution was left stirring vigorously at room temperature for 1 h. The reaction was then heated at 120 °C for 20 min and cooled. Then, AcOEt (100 mL) and water (200 mL) were added, and the resulting biphasic mixture was passed through a layer of Cellite. The organic layer was separated, and the aqueous layer was extracted with AcOEt (2 x 100 mL). The combined organic extracts were washed with sat. NaHCO_3 and dried (Na_2SO_4). The solvent was removed and the solid residue was dissolved in a MeOH/ CH_2Cl_2 mixture (1:1, 20 mL), and solid NaIO_4 (1.16 g, 5.42 mmol) was added. The mixture was stirred until the initial dihydro derivative was no longer observed by TLC (about 30 min). Inorganic salts were filtered, solvents were evaporated, and the resulting yellow solid residue was passed through a short SiO_2 column (petroleum ether/AcOEt) giving 0.659 g (3.52 mmol, 73% yield) of 3-(*tert*-butyl)benzo[*e*][1,2,4]triazine (**2b**) as a yellow microcrystalline solid: mp 72–73 °C (EtOH); ¹H NMR (CDCl_3 , 500 MHz) δ 8.49 (d, $J = 8.4$ Hz, 1H), 8.02 (d, $J = 8.5$ Hz, 1H), 7.93 (t, $J = 8.2$ Hz, 1H), 7.80 (t, $J = 7.8$ Hz, 1H), 1.63 (s, 9H); ¹³C{¹H} NMR (CDCl_3 , 125 MHz) δ 172.3, 145.9, 140.7, 135.0, 129.9, 129.5, 129.1, 39.2, 29.8. Anal. Calcd for $\text{C}_{11}\text{H}_{13}\text{N}_3$: C, 70.56; H, 7.00; N, 22.44. Found: C, 70.49; H, 7.28; N, 22.26.

Preparation of 8-substituted-1-bromonaphthalenes 3. A general procedure.

Following a literature procedure,⁵ 1,8-dibromonaphthalene (715 mg, 2.50 mmol), arylboronic acid (2.53 mmol, 1.01 equiv), Pd(PPh₃)₄ (144 mg, 0.125, 5 mol%) were dissolved in deoxygenated 1,2-dimethoxyethane (15 mL). Then, the solution of Na₂CO₃ (795 mg, 7.5 mmol, 3 equiv) in water (7 mL), which was previously purged with argon for 15 min, was added. The reaction mixture was refluxed overnight, cooled to room temperature, treated with water (15 mL) and extracted with CH₂Cl₂ (2 x 20 mL). The extract was dried (Na₂SO₄), filtered and concentrated to dryness. The resulting residue was purified by column chromatography (SiO₂, pentane) giving 8-substituted-1-bromonaphthalenes **3**.

1-Bromo-8-phenylnaphthalene (3A).⁶ Following the procedure above, 1-bromo-8-phenylnaphthalene (**3A**, 246 mg, 0.872 mmol, 35% yield) was obtained as a light yellow microcrystalline solid from 1,8-dibromonaphthalene (715 mg, 2.50 mmol) and phenylboronic acid (309 mg, 2.53 mmol): mp 37–38 °C (*n*-pentane); ¹H NMR (CDCl₃, 400 MHz) δ 7.89–7.90 (m, 2H), 7.80 (d, *J* = 7.4 Hz, 1H), 7.52 (t, *J* = 7.3 Hz, 1H), 7.45 (d, *J* = 7.0 Hz, 1H), 7.40–7.41 (m, 3H), 7.36–7.37 (m, 2H), 7.30 (t, *J* = 7.9 Hz, 1H); ¹³C{¹H} NMR (CDCl₃, 100 MHz) δ 143.0, 140.5, 136.2, 133.9, 131.3, 130.3, 129.7, 129.03, 128.98, 127.5, 127.0, 126.2, 125.4, 120.3; MS (EI) *m/z* 203 (100, [M]⁺). Anal. Calcd for C₁₆H₁₁Br: C, 67.87; H, 3.92. Found: C, 67.78; H, 4.02.

1-Bromo-8-(4-*tert*-butylphenyl)naphthalene (3B). Following the procedure above, 1-bromo-8-(4-*tert*-butylphenyl)naphthalene (**3B**, 858 mg, 2.53 mmol, 51% yield) was obtained as a white microcrystalline solid from 1,8-dibromonaphthalene (1.410 g, 4.93 mmol) and 4-*tert*-butylphenylboronic acid (885 mg, 4.97 mmol): mp 61–62 °C (EtOH); ¹H NMR (CDCl₃, 400 MHz) δ 7.95 (d, *J* = 7.4 Hz, 1H), 7.82–7.89 (m, 2H), 7.78 (d, *J* = 7.4 Hz, 1H), 7.40–7.51 (m, 4H), 7.24–7.30 (m, 2H), 1.39 (s, 9H); ¹³C{¹H} NMR (CDCl₃, 100 MHz) δ 150.2, 140.6, 139.8, 136.2, 133.8, 131.3, 129.9, 129.0, 128.8, 126.8, 126.1, 125.5, 124.4, 120.3, 34.7, 31.7; MS (EI) *m/z* 338 (40, [M]⁺). Anal. Calcd for C₂₀H₁₉Br: C, 70.80; H, 5.64. Found: C, 70.95; H, 5.39.

N^{-(2-Nitrophenyl)pivalohydrazide (5).} A solution of 1-fluoro-2-nitrobenzene (1.13 g, 9.94 mmol) and pivalohydrazide (1.41 g, 10.0 mmol, 1.01 equiv) in dry DMSO (3 mL) was stirred at 70 °C for 2 days. After cooling AcOEt (50 mL) followed by H₂O (70 mL) were added to the reaction mixture and the organic layer was separated. The aqueous layer was extracted twice with small portions of AcOEt. The combined organic layers were dried (Na₂SO₄), the solvent was evaporated, and the solid residue was recrystallized (EtOH) giving 1.15 g (4.85 mmol, 61% yield)

of hydrazide **5** as yellow microcrystalline solid: mp 143–145 °C (EtOH); ¹H NMR (DMSO-*d*₆, 500 MHz) δ 9.93 (s, 1H), 9.12 (s, 1H), 8.09 (d, *J* = 8.5 Hz, 1H), 7.59 (t, *J* = 7.8 Hz, 1H), 7.02 (d, *J* = 8.6 Hz, 1H), 6.86 (t, *J* = 7.8 Hz, 1H), 1.22 (s, 9H); ¹³C{¹H} NMR (DMSO-*d*₆, 125 MHz) δ 176.9, 145.9, 136.4, 131.8, 125.8, 117.8, 114.6, 37.6, 27.1. Anal. Calcd for C₁₁H₁₅N₃O₃: C, 55.69; H, 6.37; N, 17.71. Found C, 55.63; H, 6.48; N, 17.74.

2. NMR spectra

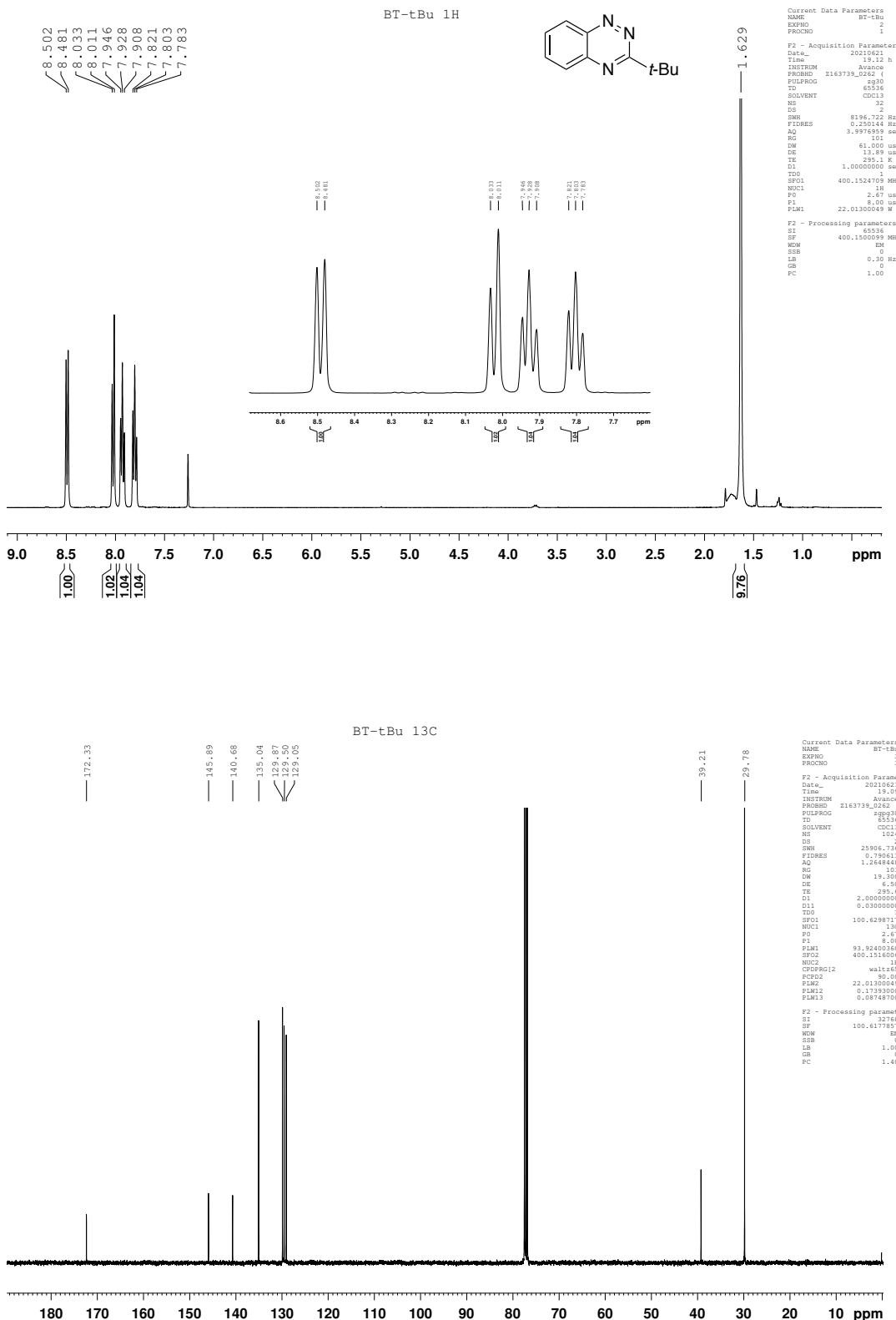


Figure S1. ^1H NMR (400 MHz) and $^{13}\text{C}\{^1\text{H}\}$ NMR (100 MHz) spectra of **2b** (CDCl_3).

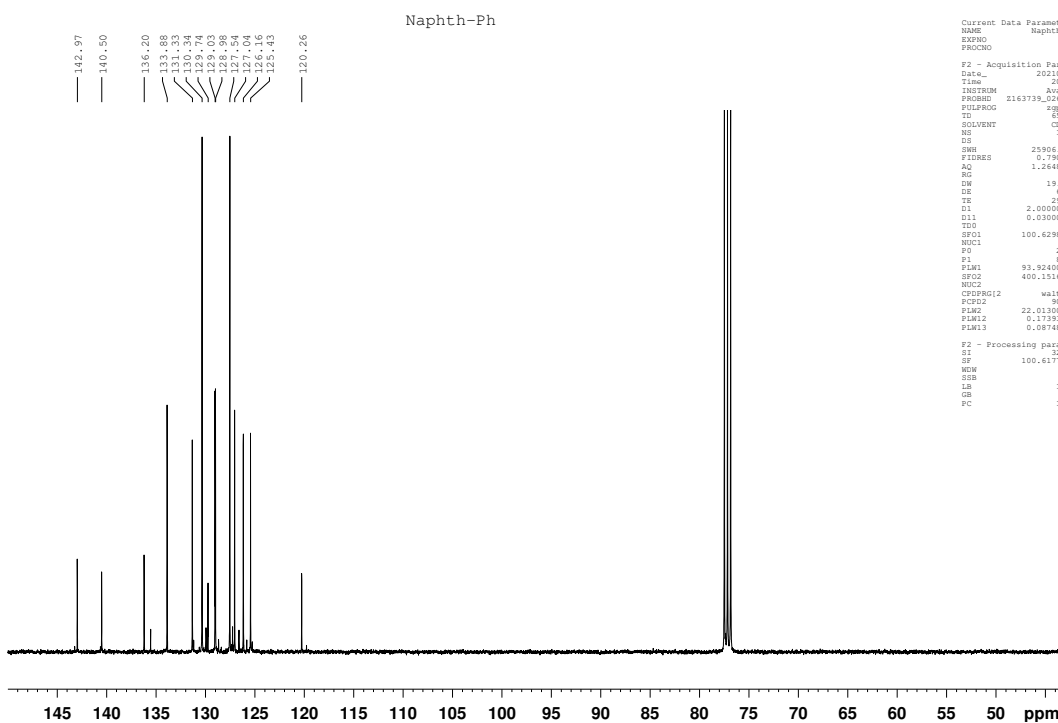
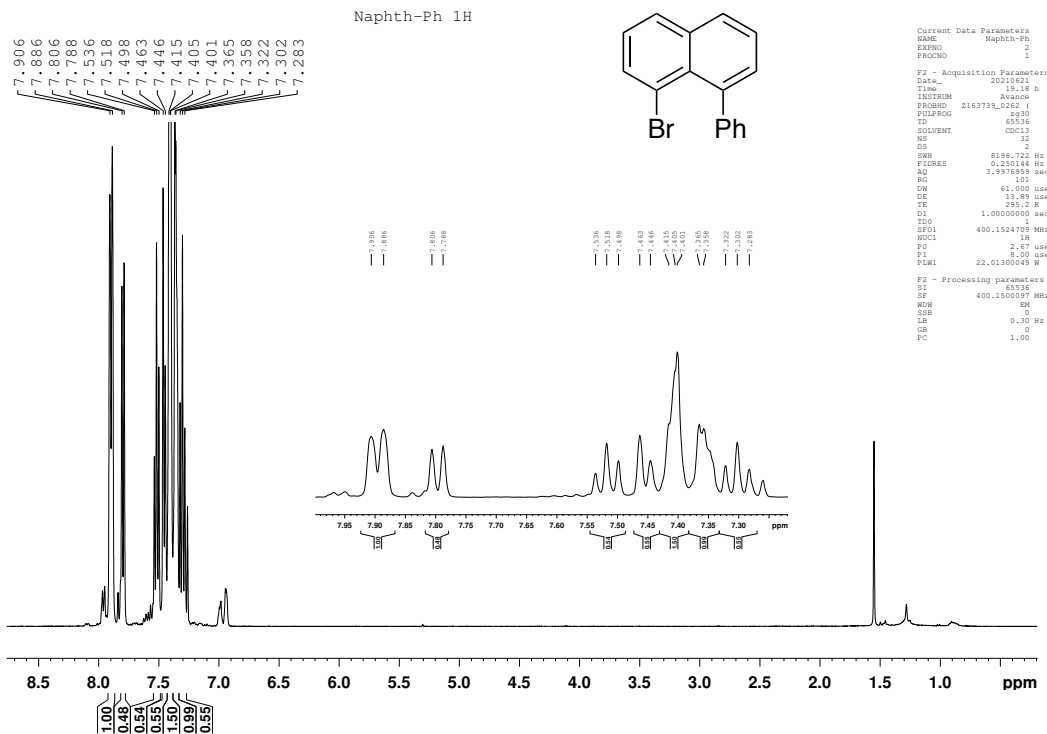


Figure S2. ^1H NMR (400 MHz) and $^{13}\text{C}\{^1\text{H}\}$ NMR (100 MHz) spectra of **3A** (CDCl_3).

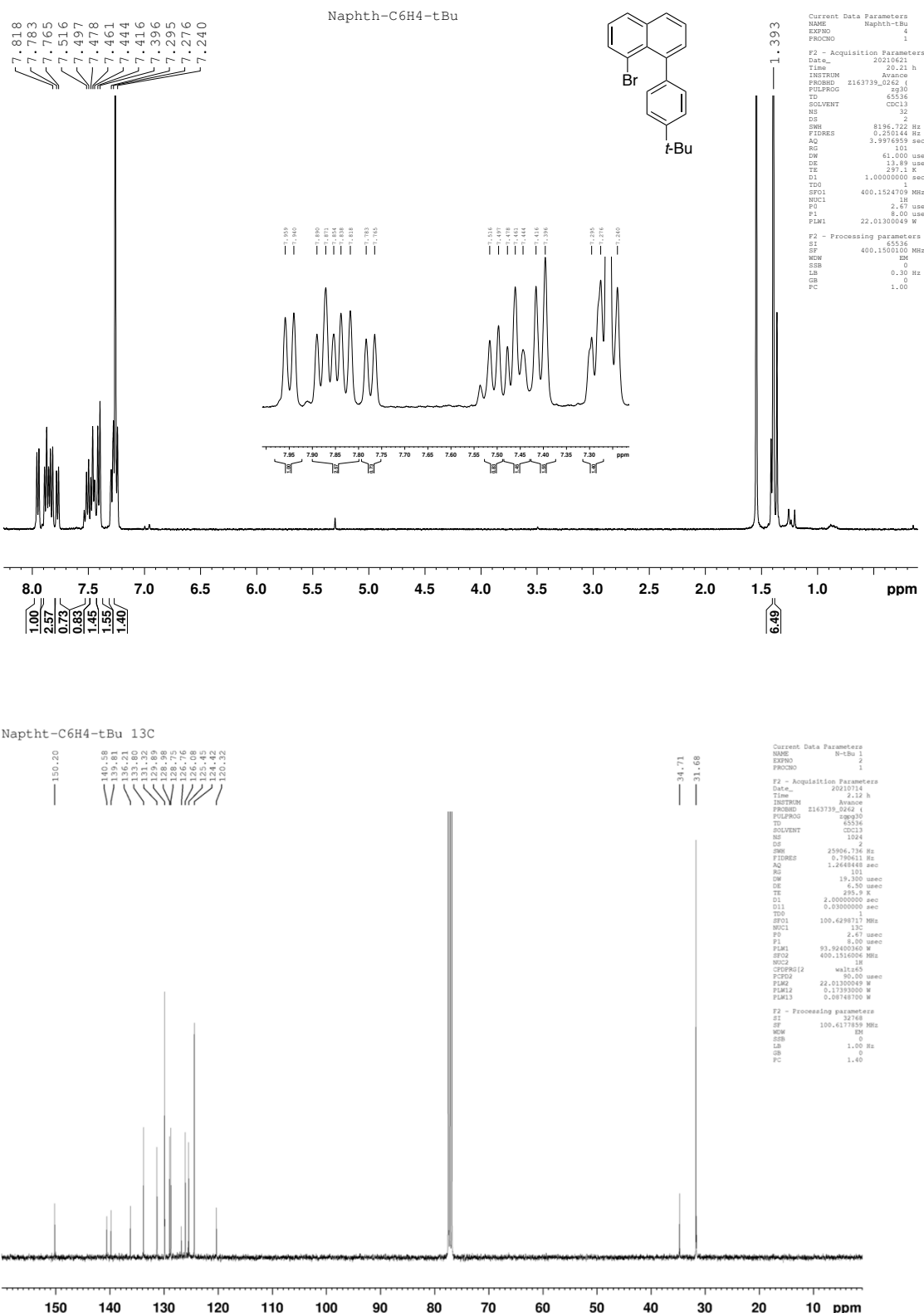


Figure S3. ^1H NMR (400 MHz) and $^{13}\text{C}\{^1\text{H}\}$ NMR (100 MHz) spectra of **3B** (CDCl_3).

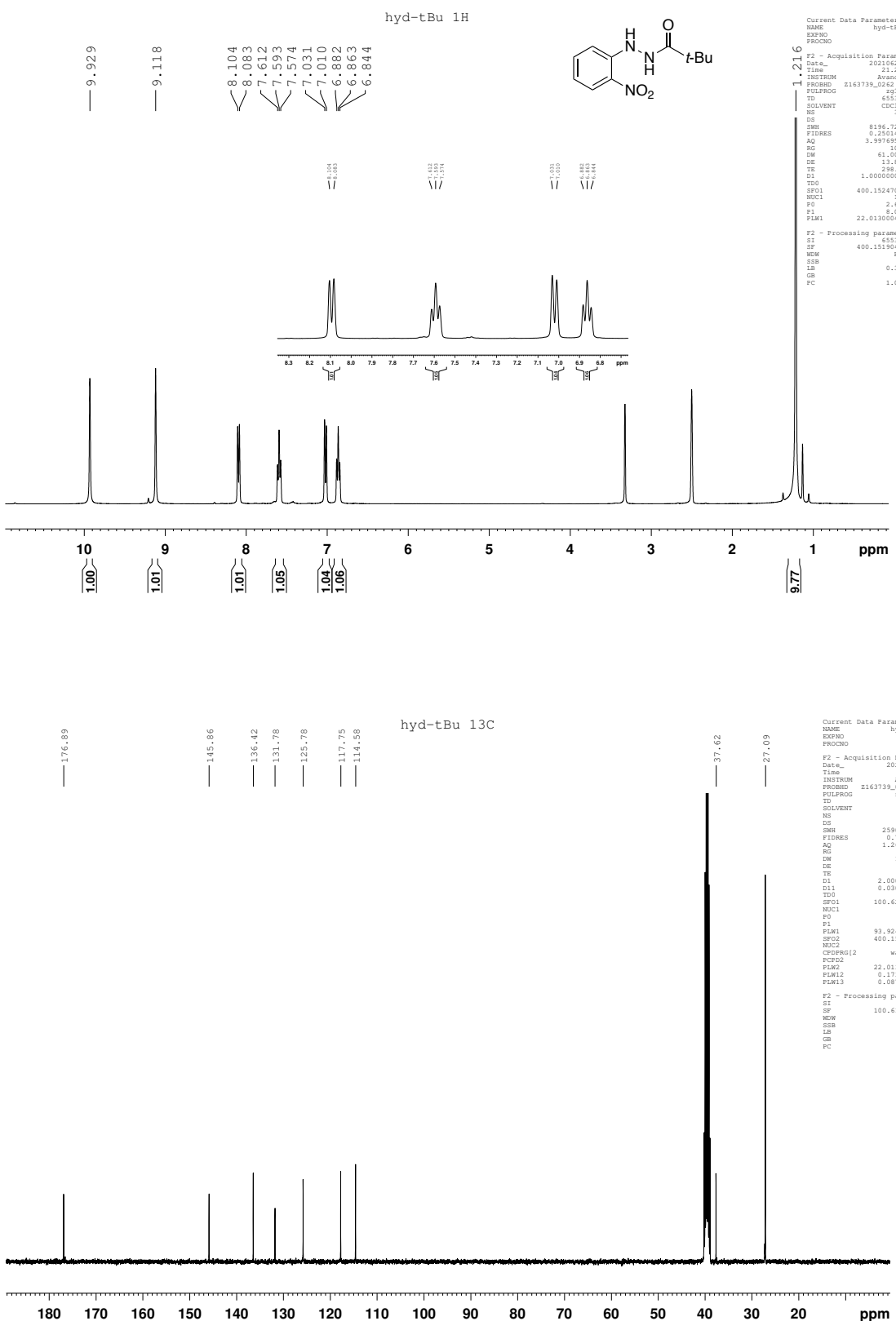


Figure S4. ^1H NMR (400 MHz) and $^{13}\text{C}\{^1\text{H}\}$ NMR (100 MHz) spectra of **5** ($\text{DMSO}-d_6$).

3. IR spectra

FT-IR spectra were recorded in KBr pellets.

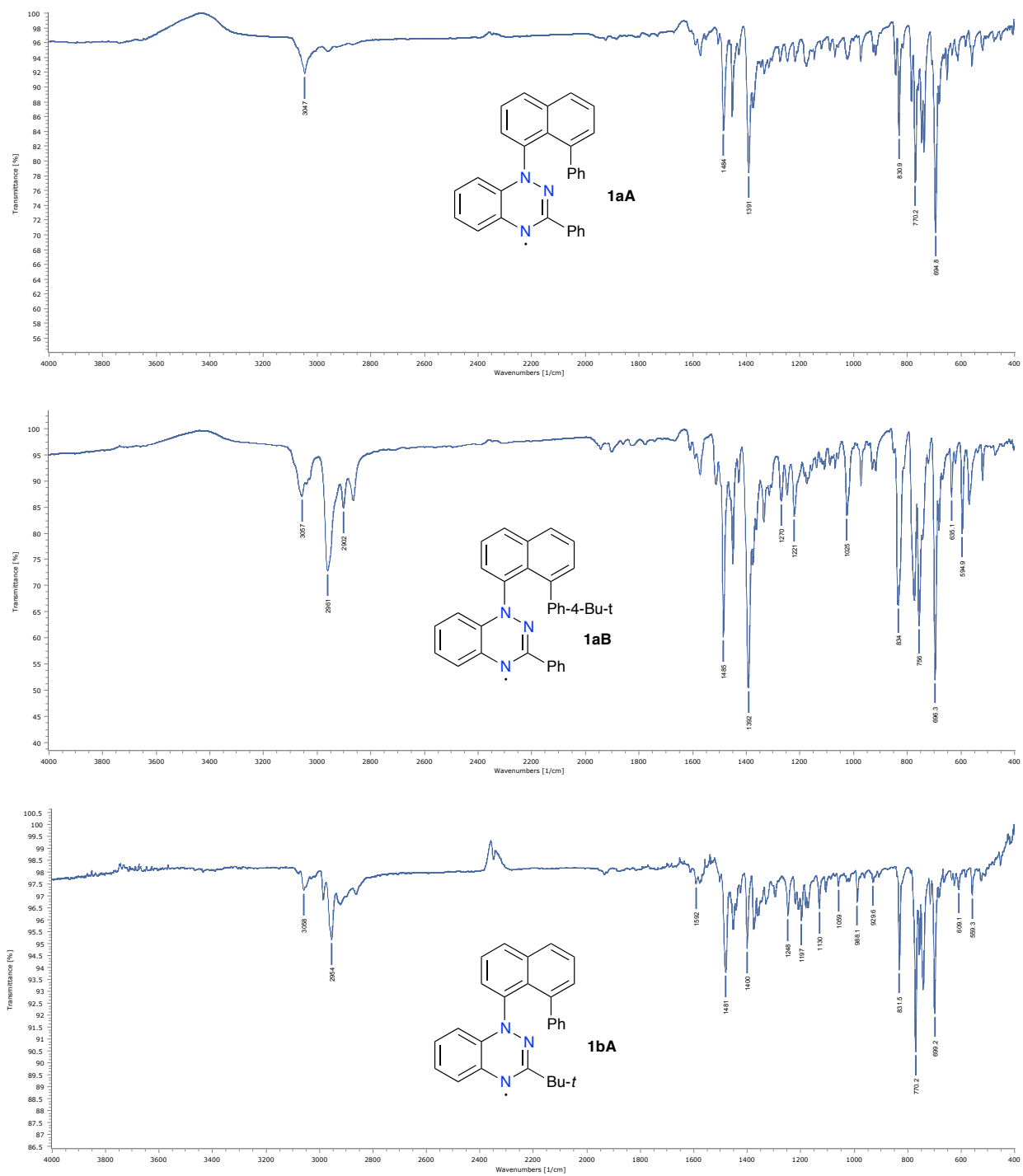


Figure S5. IR spectra for **rac-1** recorded in KBr.

4. XRD data collection and refinement

Crystals of **rac-1aA** suitable for single crystal X-ray diffraction investigation were grown by slow evaporation of EtOH solutions and were analysed using a Rigaku XtaLAB Synergy, Dualflex, Pilatus 300K diffractometer. The crystal was kept at 100.0(2) K during data collection and measurement was conducted using the CuK α radiation ($\lambda = 1.54184 \text{ \AA}$). The data were integrated using CrysAlisPro program.⁷ Intensities for absorption were corrected using SCALE3 ABSPACK scaling algorithm implemented in CrysAlisPro program.⁷ Structure was solved with the ShelXT structure solution program⁸ using Intrinsic Phasing and refined in the ShelXL by the full-matrix least-squares minimization on F^2 with the ShelXL refinement package.⁹ All non-hydrogen atoms were refined anisotropically. All hydrogen atoms were generated geometrically and refined isotropically using the riding model.

The crystal data and structure refinement descriptors are presented in Table S1, selected interatomic distances and angles are presented in Table S2, while thermal ellipsoid diagrams for single molecule of **1aA**, unit cell, and partial packing are shown in Figures S6.

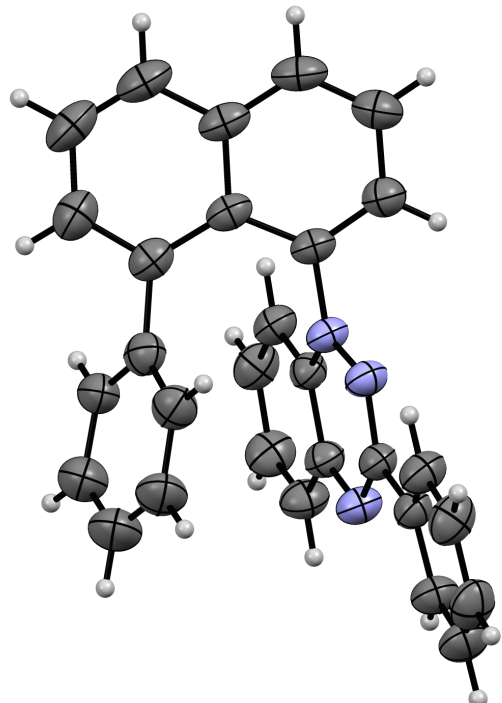
Table S1. Crystal data and refinement details for **rac-1aA**.

CDDC #	2087259
Empirical formula	C ₂₉ H ₂₀ N ₃
Formula weight	410.48
Crystal system	Triclinic
Space group	P-1
a/ Å	9.5989(2)
b/ Å	11.1996(3)
c/ Å	11.5498(3)
$\alpha/^\circ$	72.286(2)
$\beta/^\circ$	71.372(2)
$\gamma/^\circ$	65.984(2)
Volume/ Å	1056.78(5)
Z	2
Goodness-of-fit on F ²	1.085
Final R indexes [I >= 2σ (I)]	R ₁ = 0.0337, wR ₂ = 0.0945
Final R indexes [all data]	R ₁ = 0.0399, wR ₂ = 0.0985

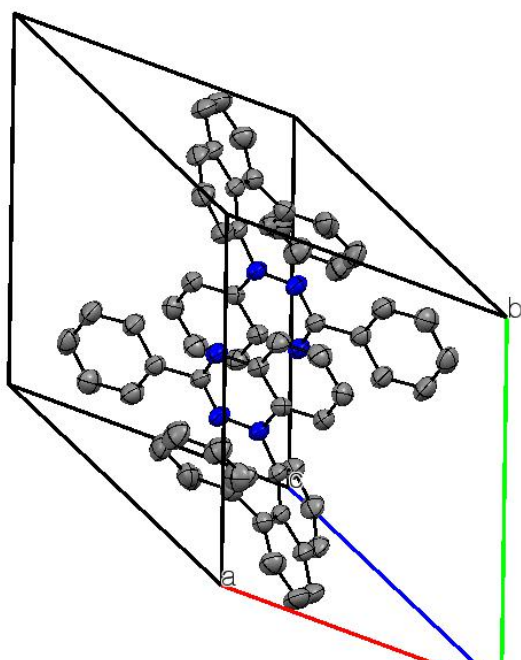
Table S2. Selected interatomic distances and angles for radical ***rac*-1aA**.^a

N(1)-Naphth	1.440(2)	C(7)-C(8)	1.373(2)
N(1)-N(2)	1.365(1)	C(8)-C(8a)	1.392(2)
N(2)-C(3)	1.336(2)	C(8a)-N(1)	1.383(1)
C(3)-N(4)	1.333(1)	C(8a)-(C4a)	1.414(2)
N(4)-C(4a)	1.372(2)	C(3)-Ph	1.489(2)
C(4a)-C(5)	1.396(1)	N(1)-N(2)-C(3)	115.44(9)
C(5)-C(6)	1.372(2)	N(2)-C(3)-N(4)	127.7(1)
C(6)-C(7)	1.392(2)		

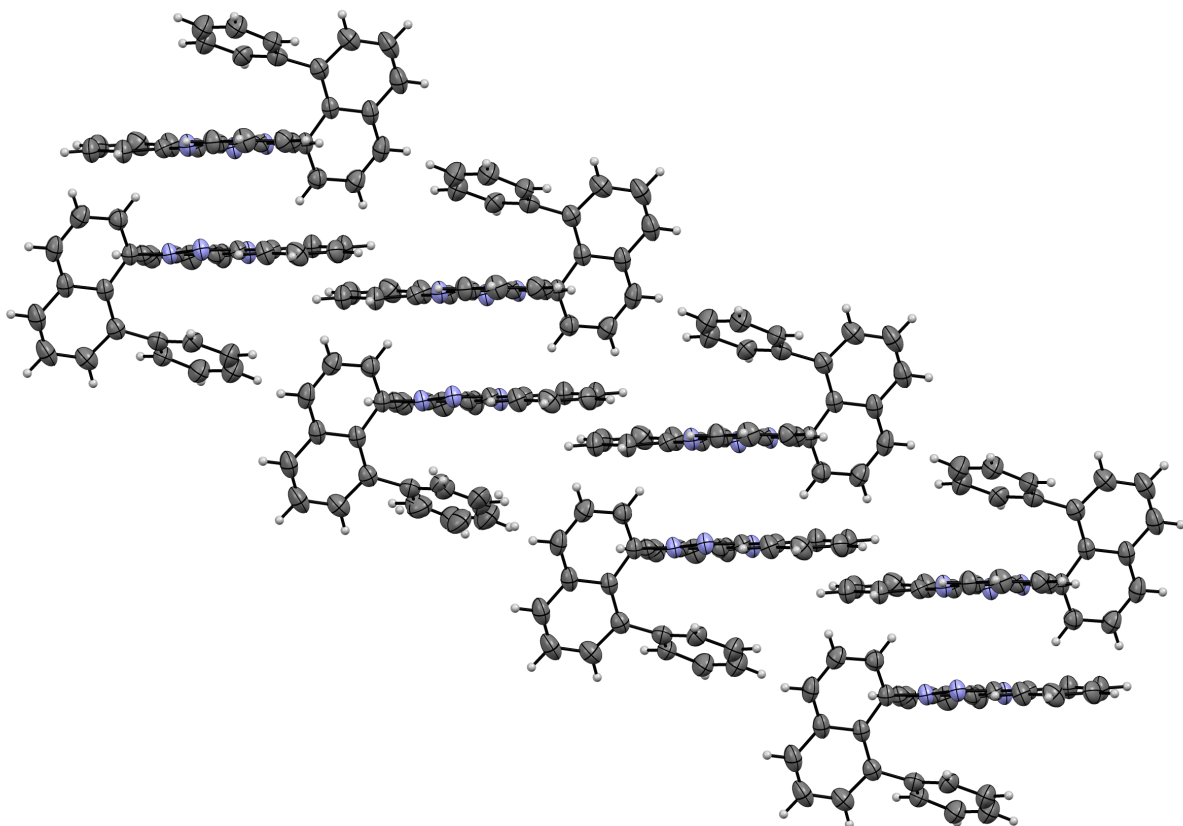
^a The numbering system according to the chemical nomenclature.



a)



b)



c)

Figure S6. Clockwise: a) thermal ellipsoid diagram for one molecule of *rac*-1aA; b) The unit cell packing diagram for *rac*-1aA (hydrogen atoms are omitted for clarity); c) partial packing diagram for *rac*-1aA. Thermal ellipsoids at 50% probability level.

5. UV-vis spectroscopy

Electronic absorption spectra for racemic radicals **rac-1** were recorded on Jasco V-770 UV-Vis-NIR spectrometer in spectroscopic grade CH_2Cl_2 at concentrations in a range $1.5\text{--}10 \times 10^{-5}$ mol/L and fitted to the Beer–Lambert law. Results are shown in Figures S7-S9.

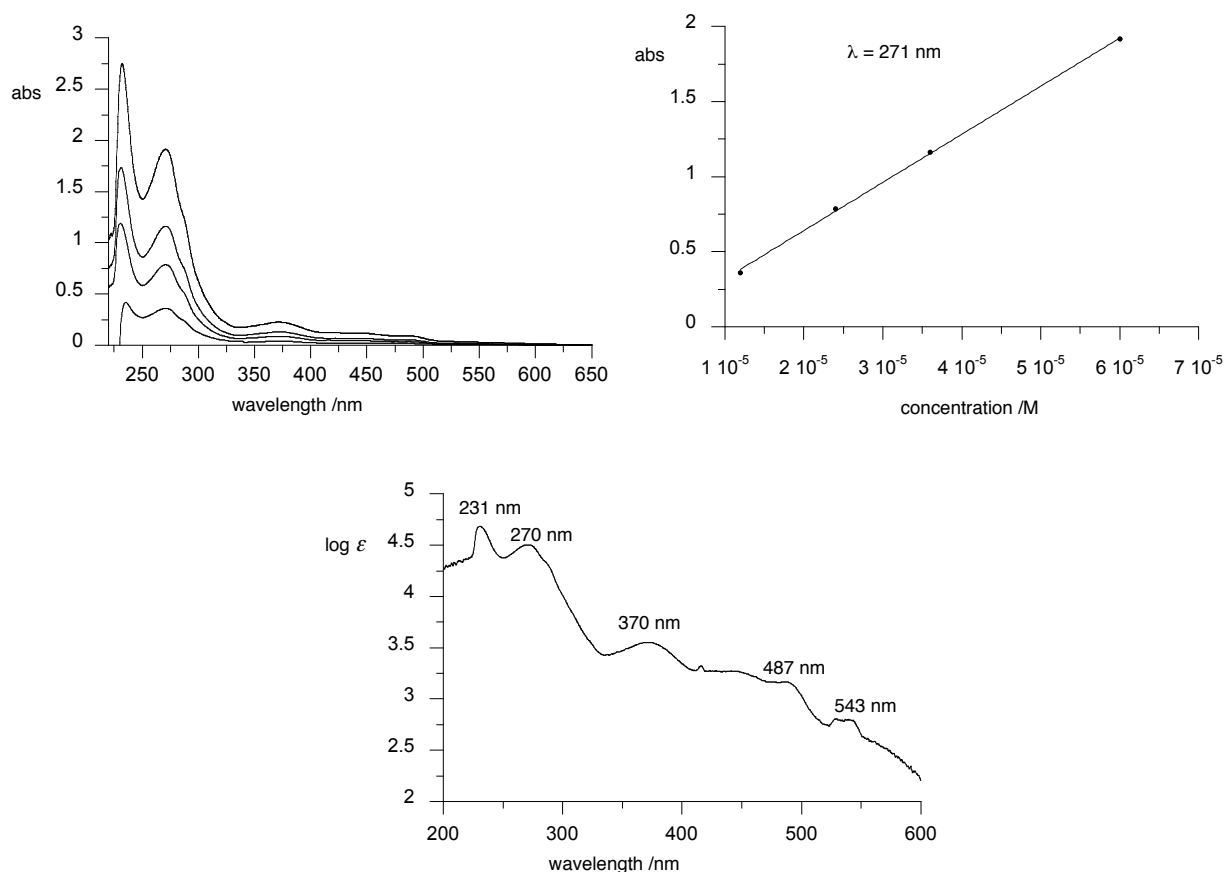
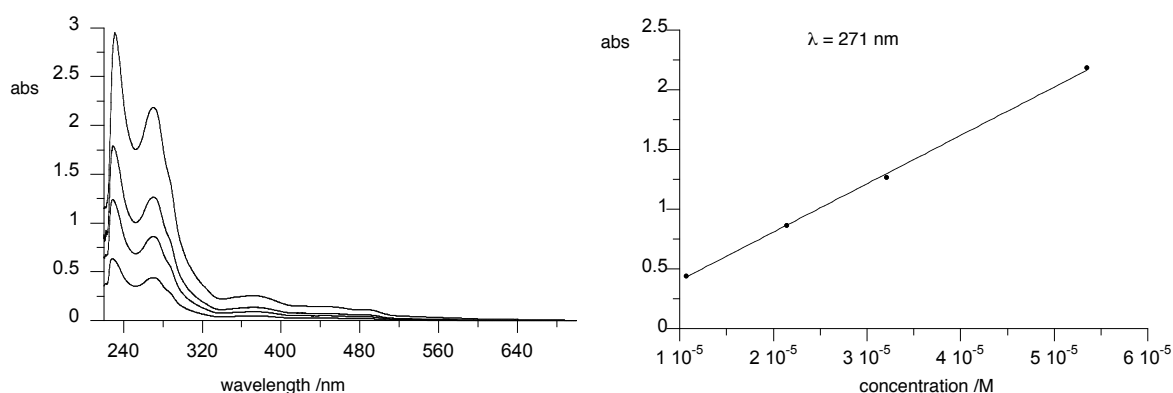


Figure S7. Clockwise: electronic absorption spectra for **rac-1aA** ($\text{R} = \text{Ph}$, $\text{X} = \text{Ph}$) in CH_2Cl_2 for four concentrations, determination of molar extinction coefficient ϵ at $\lambda = 271 \text{ nm}$ (best fit line: $\epsilon = 32057 \times \text{conc}$, $r^2 = 0.9992$), and a molar extinction $\log (\epsilon)$ plot.



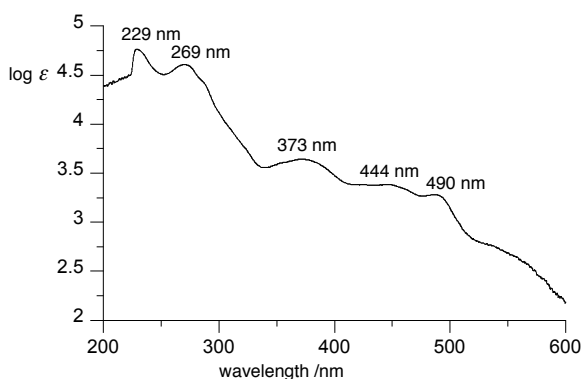


Figure S8. Clockwise: electronic absorption spectra for **rac-1aB** ($R = \text{Ph}$, $X = 4-t\text{-Bu-C}_6\text{H}_4$) in CH_2Cl_2 for four concentrations, determination of molar extinction coefficient ϵ at $\lambda = 271 \text{ nm}$ (best fit line: $\epsilon = 40436 \times \text{conc}$, $r^2 = 0.9991$), and a molar extinction $\log (\epsilon)$ plot.

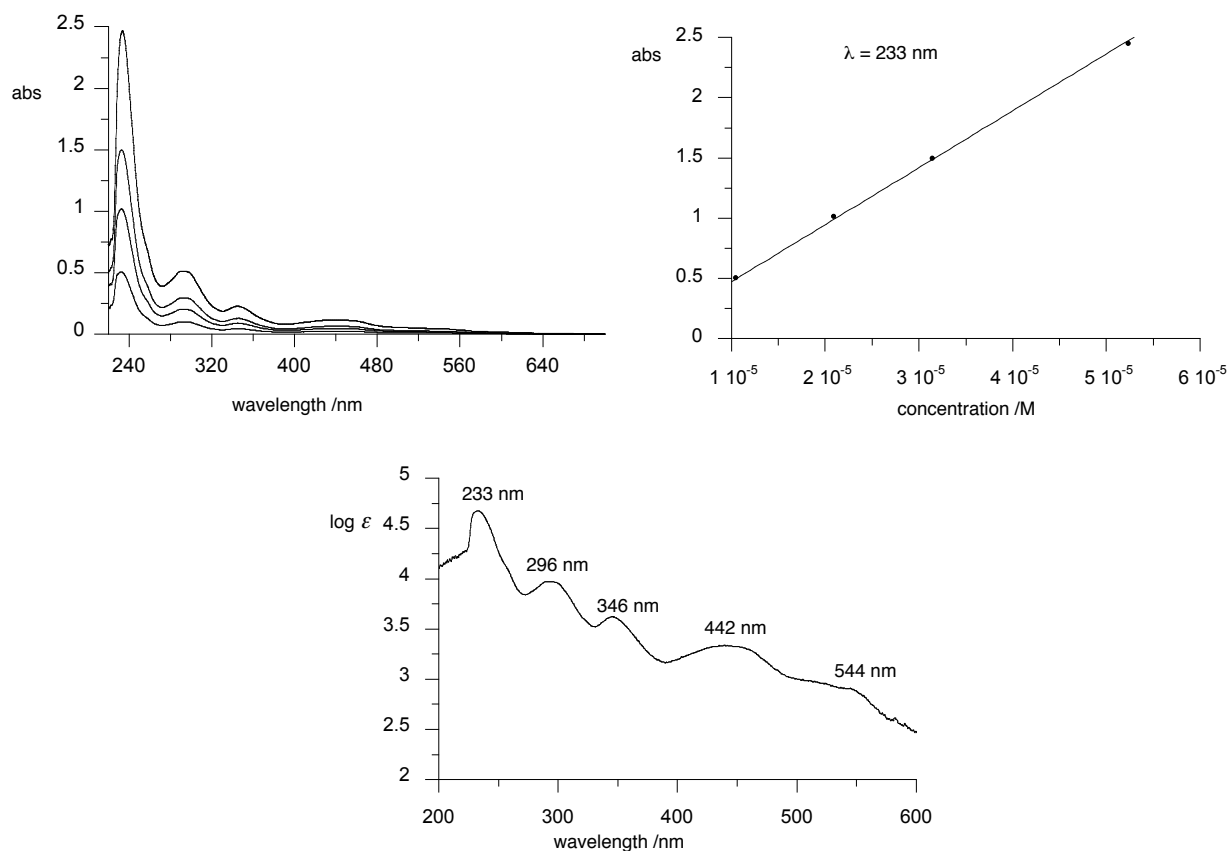


Figure S9. Clockwise: electronic absorption spectra for **rac-1bA** ($R = t\text{-Bu}$, $X = \text{Ph}$) in CH_2Cl_2 for four concentrations, determination of molar extinction coefficient ϵ at $\lambda = 233 \text{ nm}$ (best fit line: $\epsilon = 47314 \times \text{conc}$, $r^2 = 0.9992$), and a molar extinction $\log (\epsilon)$ plot.

6. EPR spectroscopy

EPR spectra for racemic radicals **rac-1** were recorded on an X-band EMX-Nano EPR spectrometer at room temperature on dilute and degassed solutions in benzene. The microwave

power was in a range of 5-15 mW (established with the Power Sweep program below the saturation of the signal) with a modulation frequency of 100 kHz, modulation amplitude of 0.5 G_{pp} and spectral width of 100 G. Accurate g-values were obtained using TEMPO as EMX-Nano internal standard. Simulations of the spectra were performed with the EMX-Nano software using DFT results (*vide infra*) as the starting point including all nitrogen and up to 4 hydrogen atoms. The resulting *hfcc* values were perturbed several times until a global minimum for the fit was achieved. Experimental and simulated spectra are shown in Figures S10–S12 and final *hfcc* are listed in Table S3.

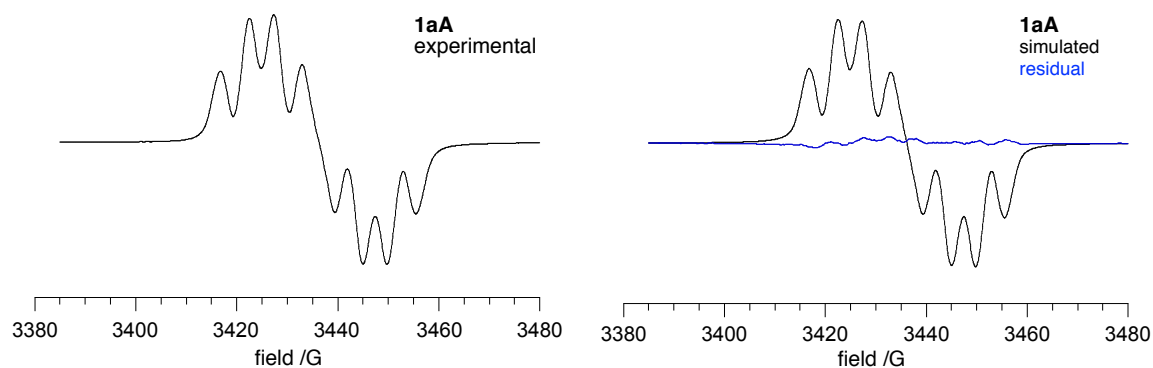


Figure S10. Experimental, simulated and difference spectra for Blatter radical ***rac-1aA*** (R = Ph, X = Ph).

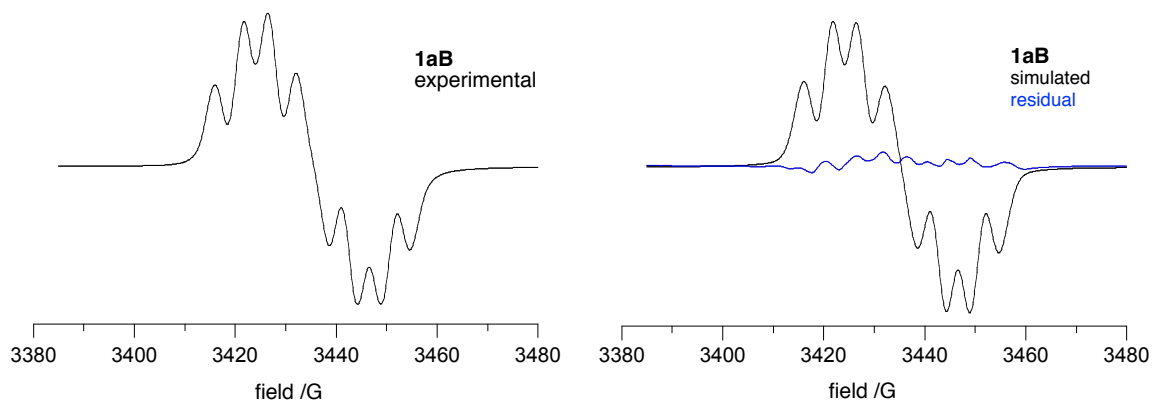


Figure S11. Experimental, simulated and difference spectra for Blatter radical ***rac-1aB*** (R = Ph, X = 4-*t*-Bu-C₆H₄).

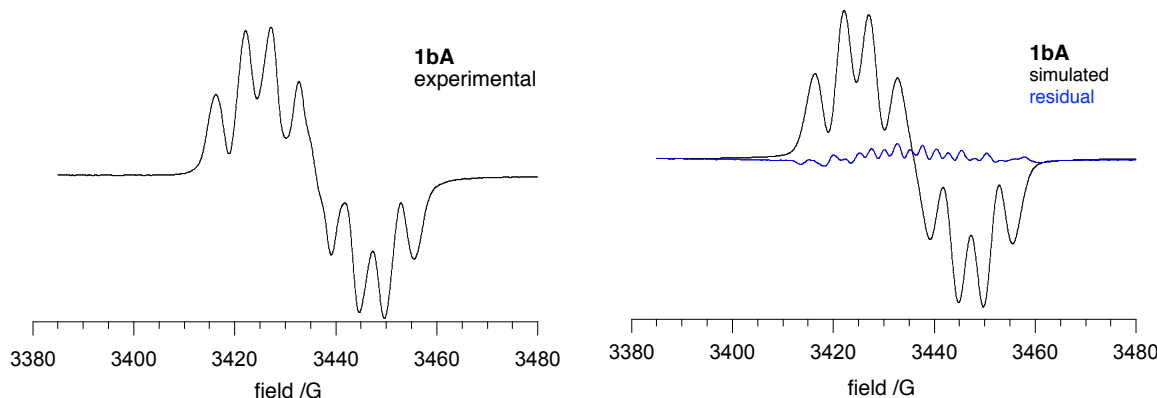
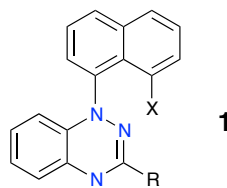


Figure S12. Experimental, simulated and difference spectra for Blatter radical ***rac-1bA*** ($R = t\text{-Bu}$, $X = \text{Ph}$).

Table S3. Summary of hyperfine coupling constants (G) for radicals ***rac-1***.^a



Compound	a_{N1}	a_{N2}	a_{N4}	a_H	a_H	a_H	a_H	g ^b
Blatter ^c	7.56	4.92	4.94	1.34	0.83	0.68	0.59	2.0036
<i>rac-1aA</i>, X = Ph, Y = Ph	7.50	4.88	5.03	1.52	1.15	1.87	0.73	2.0035
<i>rac-1aB</i>, X = <i>t</i>-Bu, Y = Ph	7.58	4.90	5.22	-	-	-	-	2.0037
<i>rac-1bA</i>, X = Ph, Y = 4-<i>t</i>-Bu-C₆H₄	7.49	4.88	5.03	0.69	0.69	0.69	0.69	2.0035

^a Assignments follow the previous EPR and ENDOR studies on ¹⁵N-labeled derivatives (ref.¹⁰). ^b Referenced to DPPH ($g = 2.0036$) as the internal standard. ^c Ref.¹¹.

7. Electrochemical results

The electrochemical characterization of racemic radicals ***rac-1*** was conducted using a Autolab PGSTAT 128N potentiostat/galvanostat in dry and degassed CH₂Cl₂ (conc. 0.5 mM) in the presence of [n-Bu₄N]⁺[PF₆]⁻ as an electrolyte (conc. 50 mM) using glassy carbon as the working electrode and Ag/AgCl pseudo reference electrode with a scan rate of 50 mV s⁻¹ at 20 °C. At the end of each measurement ferrocene was added and the peak potentials were referenced to the Fc/Fc⁺ couple (0.46 V *vs* SCE).¹²

CV plots are shown in Figures S13–S15 and numerical result are shown in Table 2 in the main text.

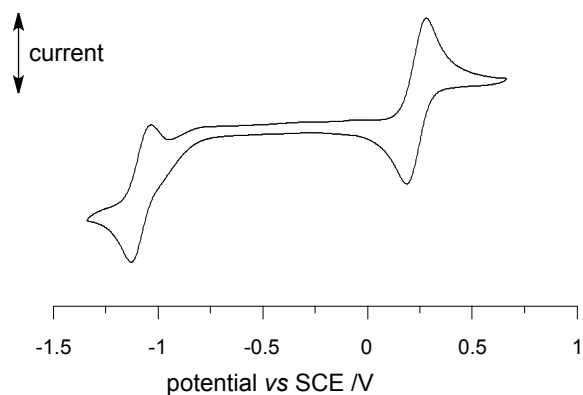


Figure S13. Cyclic voltammogram for ***rac*-1aA** ($R = \text{Ph}$, $X = \text{Ph}$).

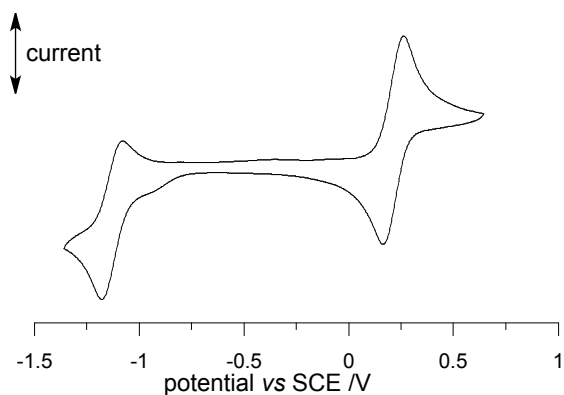


Figure S14. Cyclic voltammogram for ***rac*-1aB** ($R = \text{Ph}$, $X = 4\text{-}t\text{-BuC}_6\text{H}_4$).

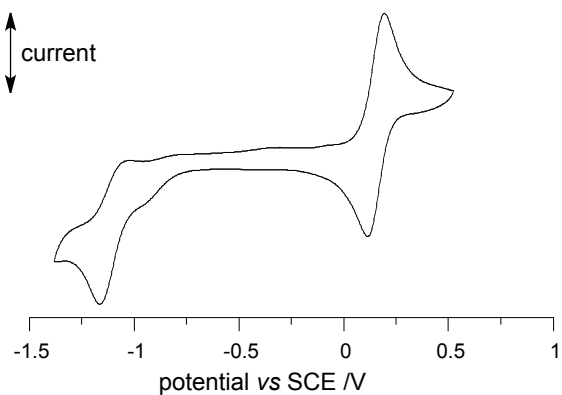


Figure S15. Cyclic voltammogram for ***rac*-1bA** ($R = t\text{-Bu}$, $X = \text{Ph}$).

8. Chiral HPLC analysis and resolution

Chiral HPLC analyses were performed on Chiralcel OD-H® analytical column (cellulose tris-3,5-dimethylphenylcarbamate, 250 × 4.6 mm) in hexane/*i*-PrOH mixtures (97:3 ratio for radicals **1aA** and **1aB**, and 99:1 ratio for radical **1bA**) at 0.5 mL/min flow and UV detection 254 nm. Retention times t_R are given in minutes. Separation of enantiomeric was accomplished on a chiral semipreparative column Lux Cellulose-1® (cellulose tris-3,5-dimethylphenylcarbamate, 250 × 10 mm) using a hexane/*i*-PrOH mixture (98:2 ratio) as the liquid phase with the flow of 3.0 mL/min and UV detection at 254 nm.

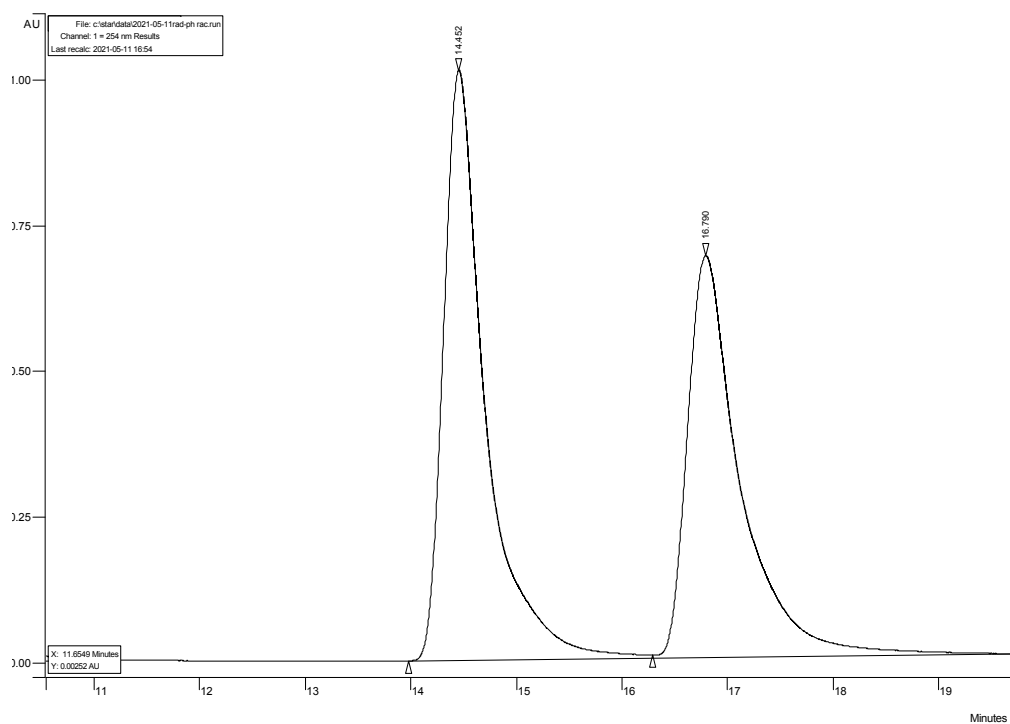


Figure S16. Chiral HPLC analysis of racemic radical **rac-1aA** ($R = Ph$, $X = Ph$) using Chiralcel OD-H® analytical column. Hexane/*i*-PrOH 97:3 ratio.

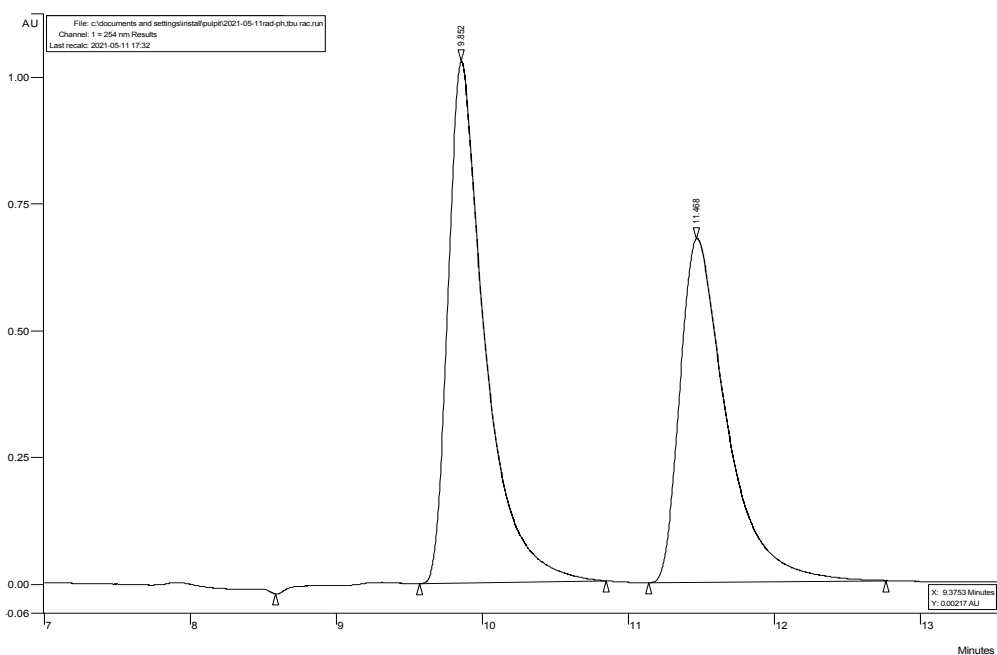


Figure S17. Chiral HPLC analysis of racemic radical **rac-1aB** ($R = \text{Ph}$, $X = 4-t\text{-BuC}_6\text{H}_4$) using Chiralcel OD-H® analytical column. Hexane/*i*-PrOH 99:1 ratio.

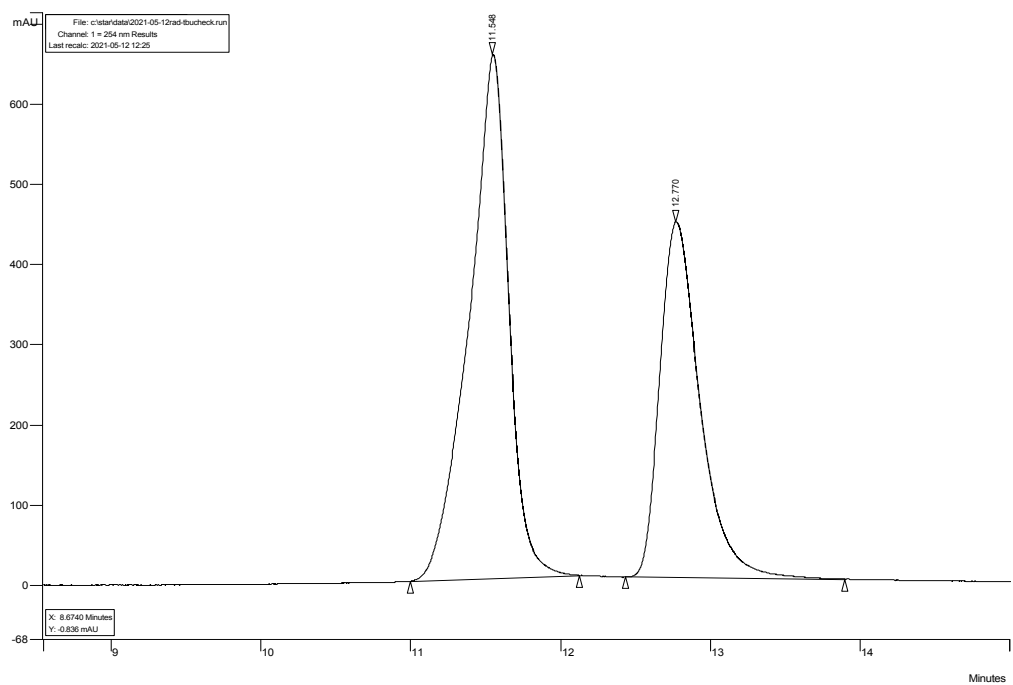


Figure S18. Chiral HPLC analysis of racemic radical **rac-1bA** ($R = t\text{-Bu}$, $X = \text{Ph}$) using Chiralcel OD-H® analytical column. Hexane/*i*-PrOH 97:3 ratio.

9. Optical rotation

Determination of specific rotation of individual atropisomers was attempted using Perkin Elmer 241MC polarimeter in CH_2Cl_2 solutions. High optical density of the solutions and consequently low concentrations of the analyte resulted in unreliable measurement in a range 550–800 nm. The analysis gave only the sign of the optical rotation listed in Table S4.

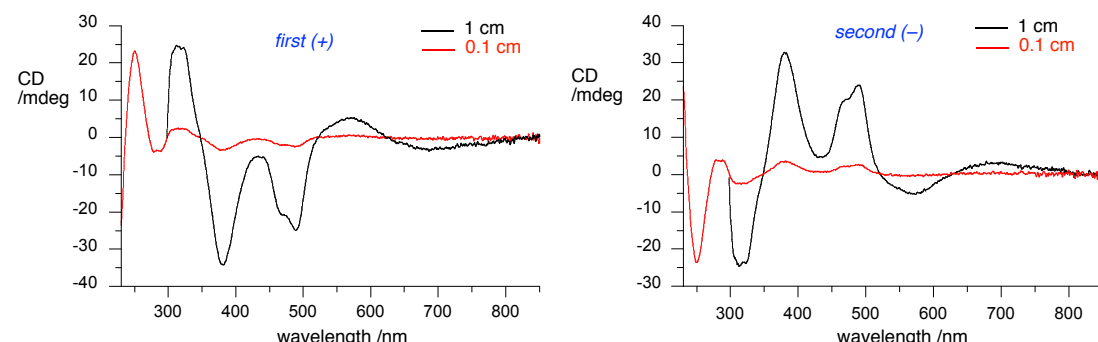
Table S4. Optical rotation sign for atropisomers **1** in CH_2Cl_2 .

Compound	Fraction	
	<i>first</i> ^[a]	<i>second</i> ^[b]
1aA X = Ph, Y = Ph	(+)	(-)
1aB X = <i>t</i> -Bu, Y = Ph	(+)	(-)
1bA , X = Ph, Y = 4- <i>t</i> -Bu-C ₆ H ₄	(+)	(-)

^[a] Shorter retention time. ^[b] Longer retention time.

10. Electronic circular dichroism spectroscopy

Electronic circular dichroism spectra of individual atropisomers **1** were recorded on Jasco J-1500 CD spectrometer in spectroscopic grade CH_2Cl_2 , in 1.0 and 0.1 cm cuvettes, at concentrations in a range $2\text{--}3 \times 10^{-4}$ mol/L. Results are shown in Figures S19–S21. The notation *first* and *second* refers to the shorter and longer retention times, respectively, of the individual atropisomers. The sign was determined with polarimetric methods (*vide supra*).



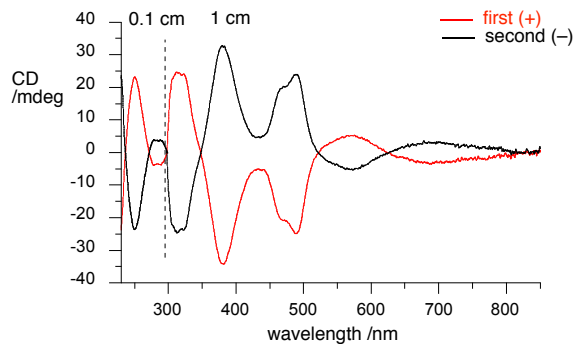


Figure S19. Clockwise: electronic circular dichroism spectra for *the first* (+) ($c = 2.66 \times 10^{-4}$ mol L $^{-1}$) and *the second* (-) ($c = 2.64 \times 10^{-4}$ mol L $^{-1}$) atropisomers of radical **1aA** (R = Ph, X = Ph) in CH₂Cl₂ in 1 cm (black lines) and 0.1 cm (red lines) cuvettes, combined ECD spectra of both atropisomers.

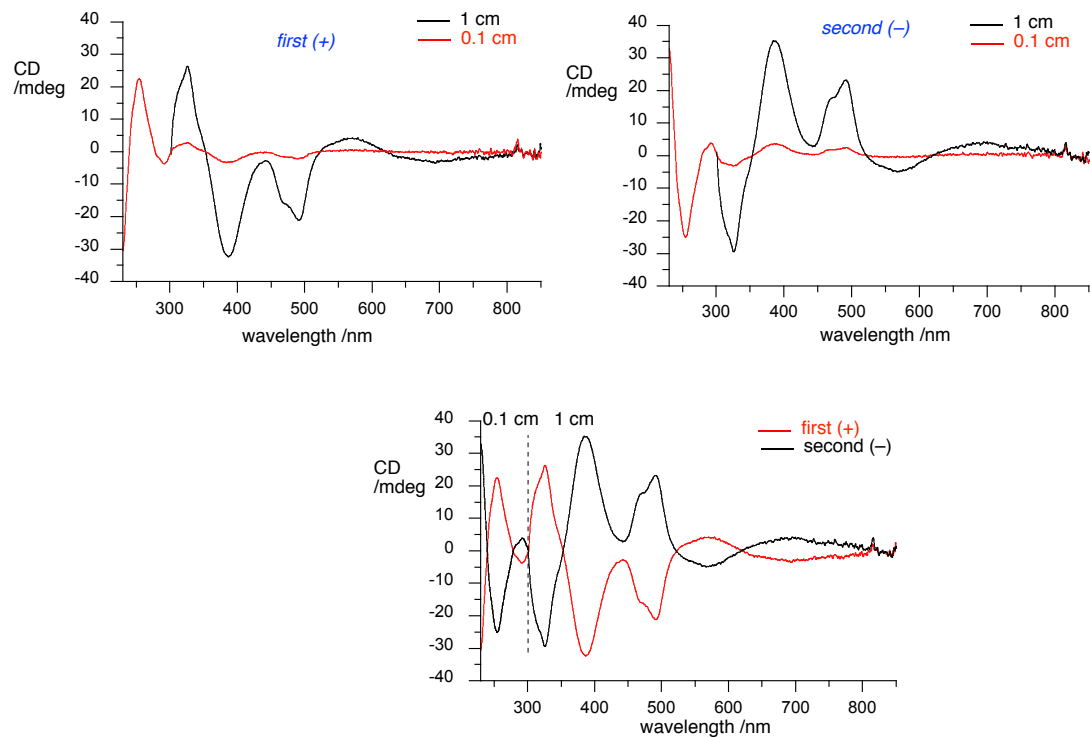


Figure S20. Clockwise: electronic circular dichroism spectra for *the first* (+) ($c = 2.82 \times 10^{-4}$ mol L $^{-1}$) and *the second* (-) ($c = 2.77 \times 10^{-4}$ mol L $^{-1}$) atropisomers of radical **1aB** (R = Ph, X = 4-*t*-BuC₆H₄) in CH₂Cl₂ in 1 cm (black lines) and 0.1 cm (red lines) cuvettes, combined ECD spectra of both atropisomers.

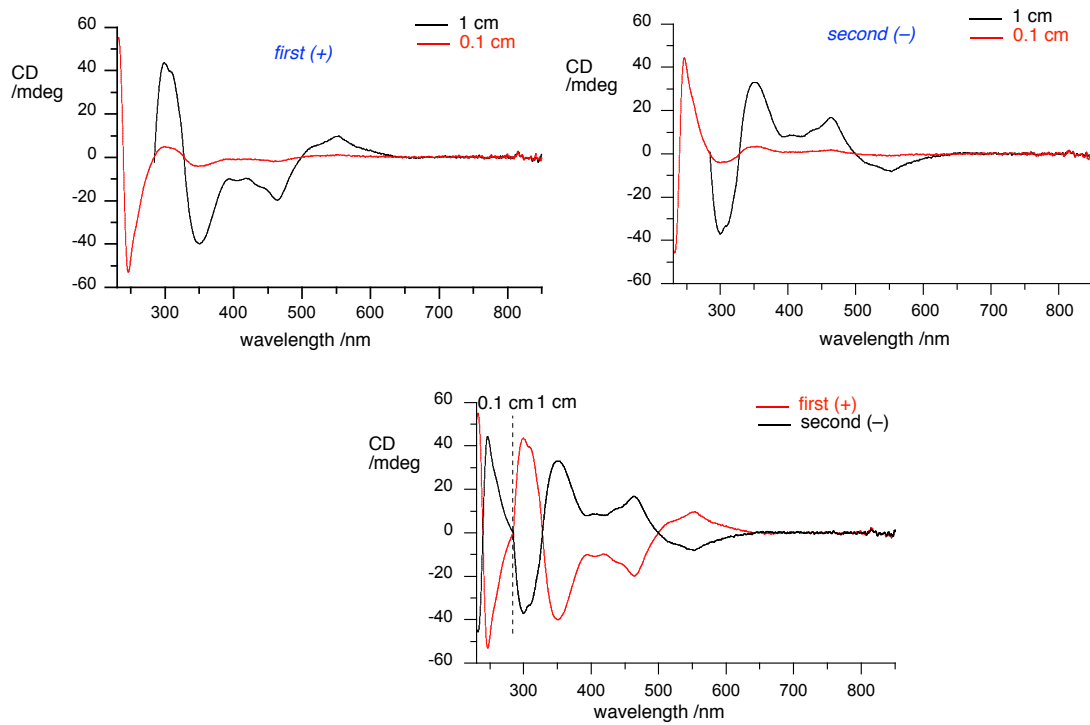


Figure S21. Clockwise: electronic circular dichroism spectra for *the first* (+) ($c = 2.29 \times 10^{-4}$ mol L $^{-1}$) and *the second* (-) ($c = 2.25 \times 10^{-4}$ mol L $^{-1}$) atropisomers of radical **1bA** ($R = t\text{-Bu}$, $X = \text{Ph}$) in CH_2Cl_2 in 1 cm (black lines) and 0.1 cm (red lines) cuvettes; combined ECD spectra of both atropisomers.

11. Determination of absolute configuration of the atropisomers

The absolute configuration was assigned to radical atropisomers **1** by comparison of experimental and DFT calculated electronic circular dichroism (ECD) spectra. Theoretical ECD spectra were obtained at the UCAM-B3LYP/Def2SVP // UB3LYP/Def2SVP level of theory in CH_2Cl_2 dielectric medium using the PCM model requested with SCRF(solvent=CH2CL2) keyword, with TD method and 45 or 50 states. Results are shown in Figures S22–S27.

ECD spectra were processed using UV peak half-width at high height set at 0.170 eV

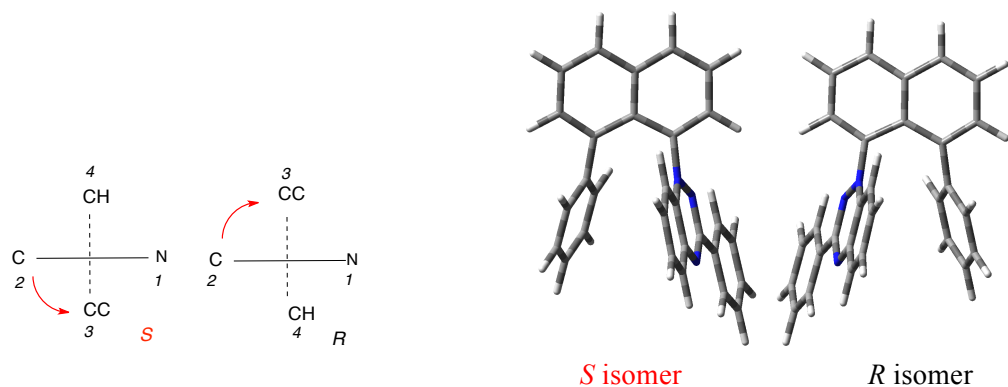


Figure S22. Left: a general scheme for assignment of absolute configuration in series **1**. Right: *S* and *R* atropisomers of radical **1aA**.

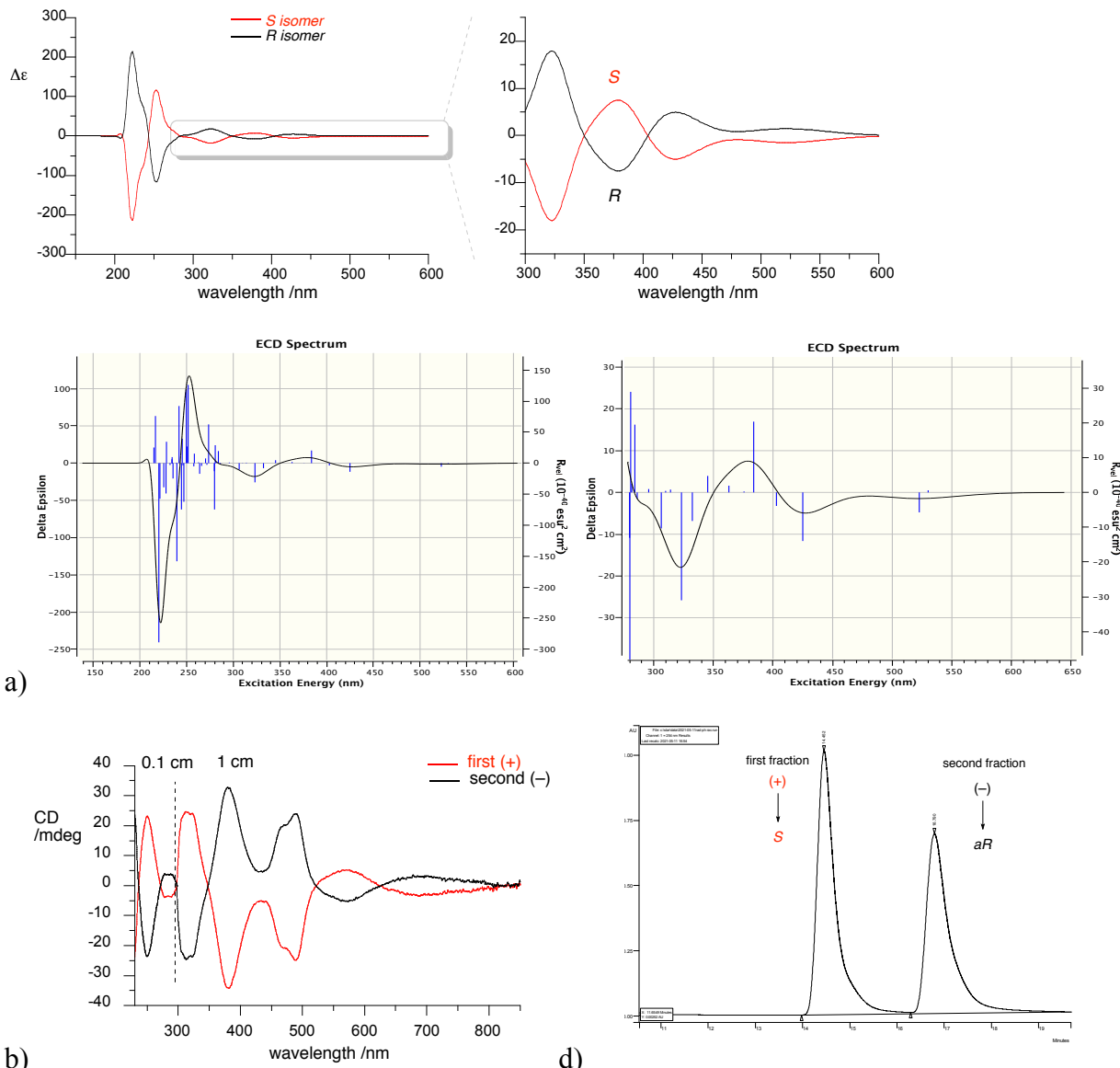
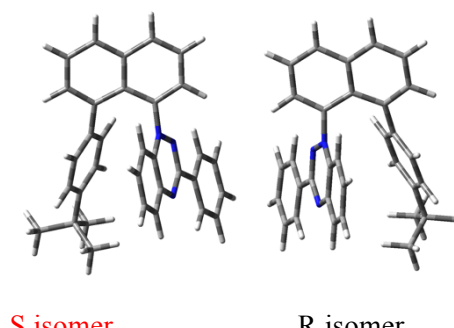


Figure S23. ECD spectra of **1aA** atropisomers *R* (black line) and *S* (red line): a) TD-DFT calculated and b) measured in CH_2Cl_2 ; c) chiral HPLC analysis of radical *rac*-**1aA** and absolute configuration assignment.

Radical **1aB** ($\text{R} = \text{Ph}$, $\text{X} = 4-t\text{-Bu-C}_6\text{H}_4$)



S isomer

R isomer

Figure S24. Configuration of *S* and *R* atropisomers of radical **1aB**.

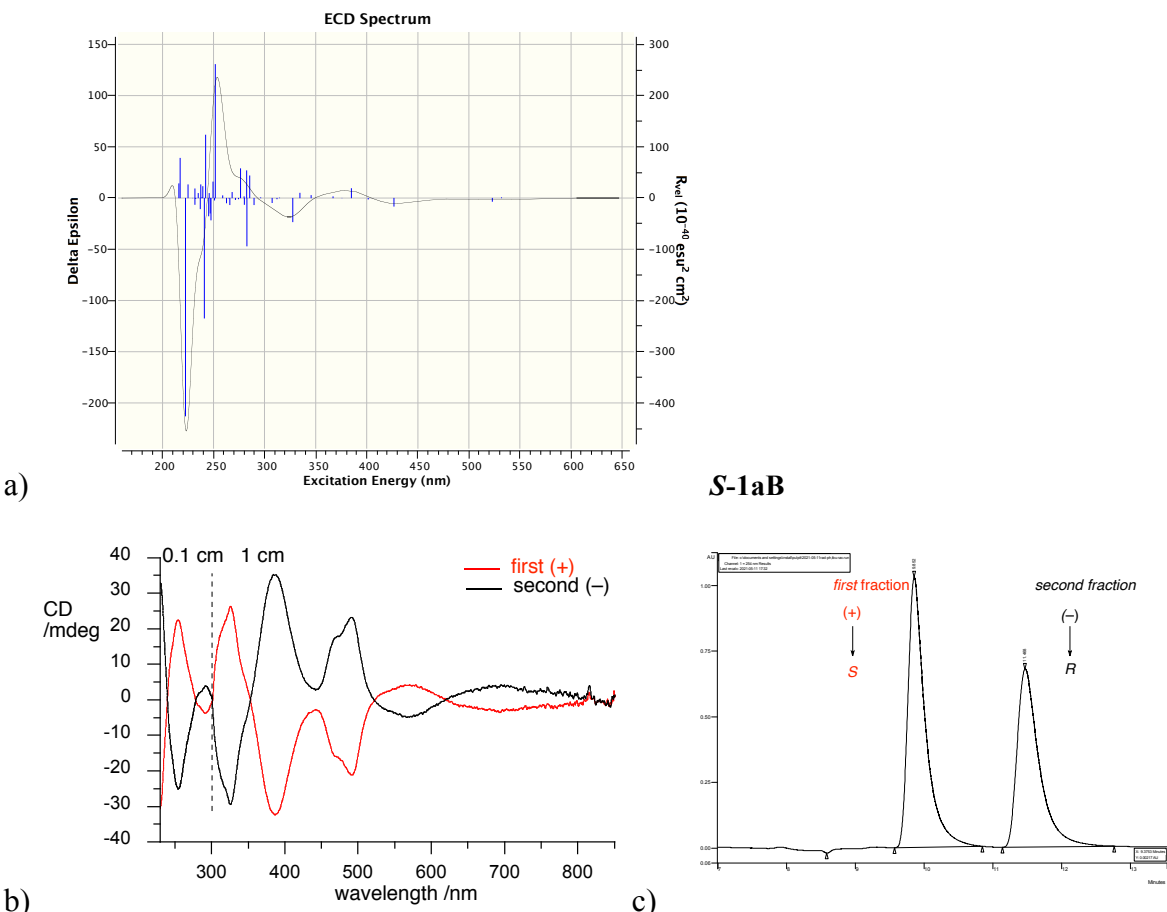
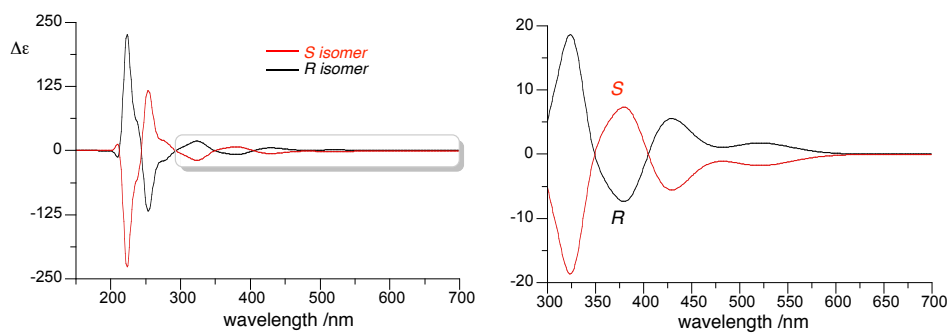


Figure S25. ECD spectra of **1aB** atropisomers *R* (black line) and *S* (red line): a) TD-DFT calculated and b) measured in CH_2Cl_2 ; c) chiral HPLC analysis of radical *rac*-**1aB** and absolute configuration assignment.

Radical 1bA ($R = t\text{-Bu}$, $X = \text{Ph}$) 45 states,

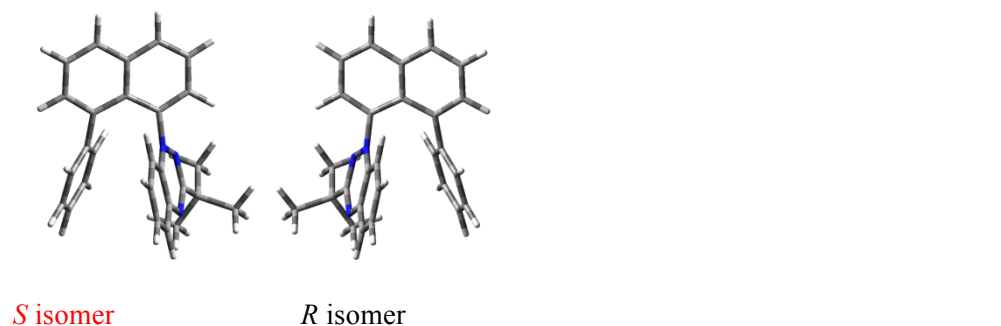
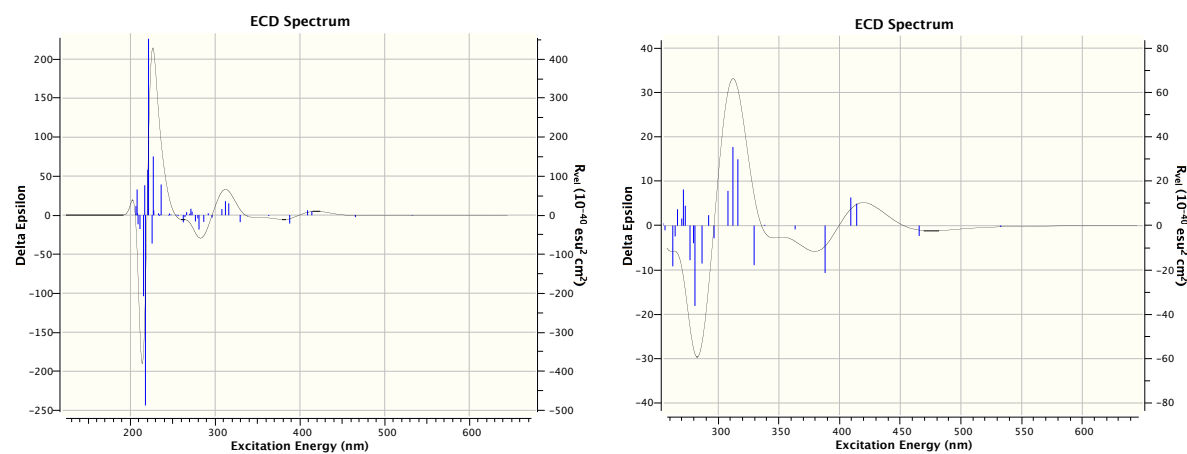
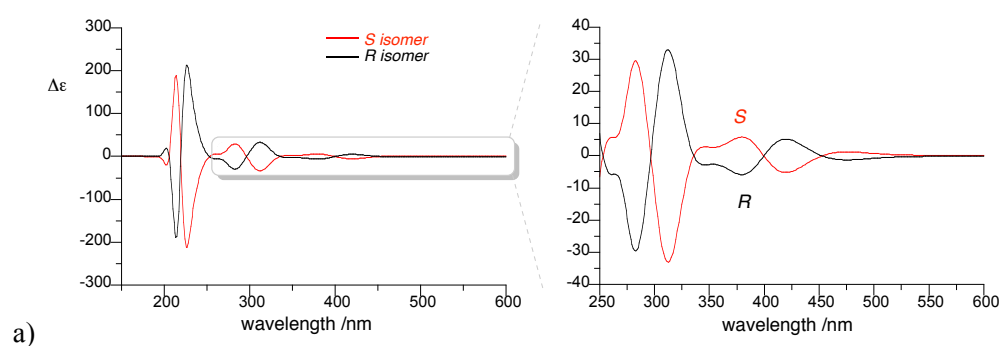
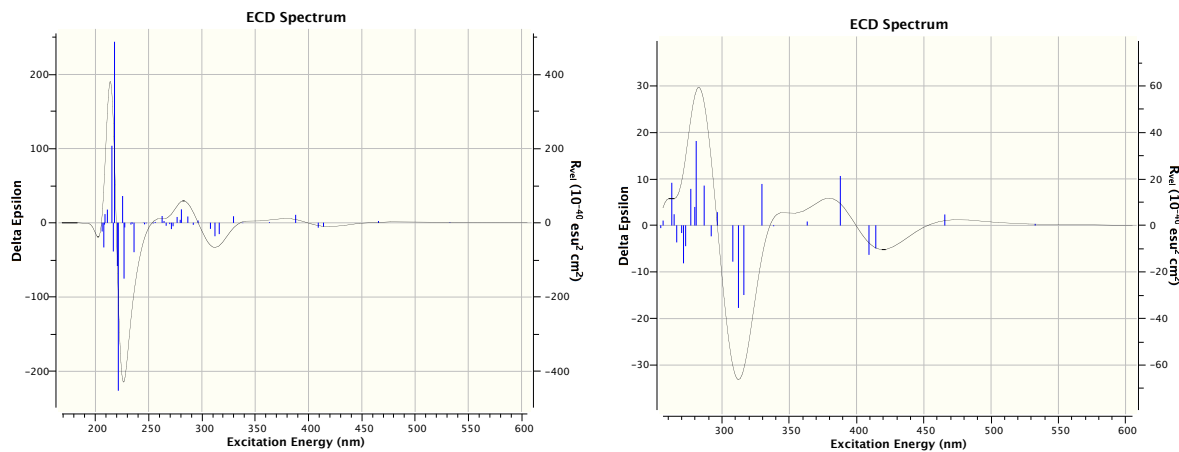
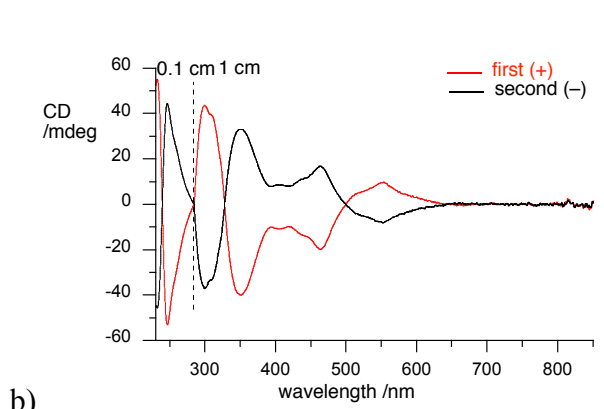


Figure S26. Configurations of *S* and *R* atropisomers of radical **1bA**.

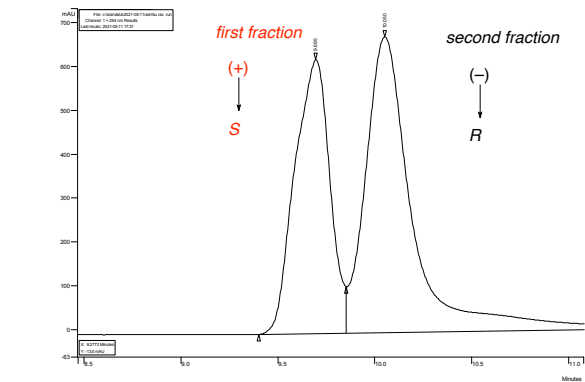




a) **S-1bA**



b)



c)

Figure S27. ECD spectra of **1bA** atropisomers *R* (black line) and *S* (red line): a) TD-DFT calculated and b) measured in CH_2Cl_2 ; c) chiral HPLC analysis of radical *rac-1bA* and absolute configuration assignment.

12. Kinetics analysis of racemization

All kinetic experiments were conducted in a closed vessel in 1,2-dichloroethane or cyclohexane. The temperature was controlled using Thermo Scientific dry bath thermostat. For kinetics experiments carried out in 1,2-dichloromethane, samples (15 μL) were withdrawn at fixed time intervals (5, 10, 15 or 20 min), diluted with hexane (30 μL) and then cooled to 0 °C. The *ee* variation as a function of time was monitored by chiral HPLC (Chiralcel OD-H, hexane/*i*-PrOH, 97:3 ratio for radicals **1aA** and **1aB**, and hexane/*i*-PrOH 99:1 ratio for radical **1bA**, flow 0.5 mL/min). For kinetic experiments carried out in cyclohexane, samples were withdrawn at fixed time intervals (5, 10, 15 or 20 min), cooled to 0 °C, and then analyzed by chiral HPLC as described above without dilution with hexane. The rate constant of enantiomerization, k_{en} , was determined from first order kinetic line fitting according to equation 1:¹³

$$\ln ee = -2k_{en}t + C \quad \text{eq 1}$$

where ee is an enantiomeric excess defined as $(1-R/S)/(1+R/S)$, k_{en} is the rate constant of enantiomer interconversion (s^{-1}) and t is the racemization time (s).

For calculation of activation parameters frequently is used the racemization rate constant k_{rac} , which is related to k_{en} by $k_{rac} = 2 \times k_{en}$.¹³ The constant k_{rac} is appropriate, however for irreversible processes, not for equilibrium processes, such as this one. Thus, further analyses were conducted using the enantiomer interconversion rate constant, k_{en} . The use of the k_{rac} constant instead of k_{en} affects only the ΔS^\ddagger by $+1.4 \text{ cal mol}^{-1} \text{ K}^{-1}$, which consequently lowers the ΔG_{298}^\ddagger by $0.42 \text{ kcal mol}^{-1}$.

The half-life of racemization, $t_{1/2\text{rac}}$, the time during which the enantiomeric excess is reduced to 50%, was calculated using equation 2:

$$t_{1/2\text{rac}} = \frac{\ln 2}{2k_{en}} = \frac{\ln 2}{k_{rac}} \quad \text{eq 2}$$

The experimentally obtained k_{en} values were analyzed using the Arrhenius equation 3:

$$\ln k_{en} = \ln A - \frac{E_a}{RT} \quad \text{eq 3}$$

where A is the frequency factor, E_a is activation energy of enantiomerization, R is the gas constant and T absolute temperature. The value for E_a and $\ln A$ were determined from a $\ln k_{en}$ ($1/T$) plot.

Temperature-independent thermodynamic parameters ΔH^\ddagger and ΔS^\ddagger were determined from the Eyring plot according to equation 4:

$$\ln \left(\frac{k_{en}}{T} \right) = -\frac{\Delta H^\ddagger}{RT} + \ln \left(\frac{k_B}{h} \right) + \frac{\Delta S^\ddagger}{R} \quad \text{eq 4}$$

Finally, the apparent free energy barrier (ΔG_T^\ddagger) of enantiomer interconversion was calculated according to equation 5:

$$\Delta G_T^\ddagger = \Delta H^\ddagger - T\Delta S^\ddagger \quad \text{eq 5}$$

where T is taken as standard temperature (298 K).

Confidence interval, CI, was determined for each parameter using equation 6:

$$CI = 2 \times R \times z \frac{std}{\sqrt{n}} \quad \text{eq 6}$$

for which confidence z was taken as 95% and R is the gas constant.

The first order kinetics data of racemization of enantiopure radicals **1** are shown at Figures S28-S37 and resulting k_{en} and racemization activation parameters are presented in Tables S5 and S6.

Plotting and statistical analysis were performed with KaleidaGraph 4.5.0 software.

Kinetics data of racemization in 1,2-dichloroethane

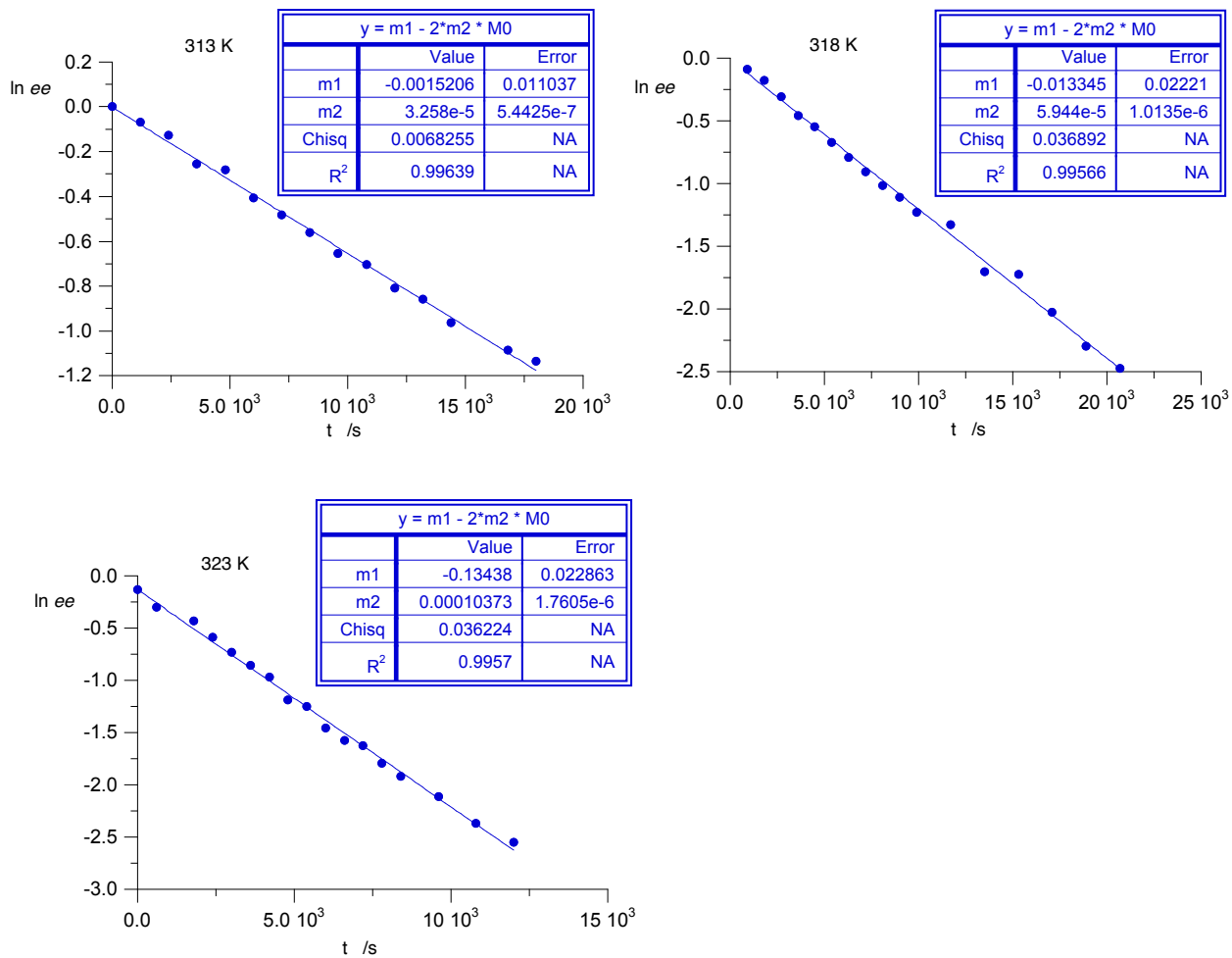


Figure S28. First order kinetics for racemization of radical **1aA** in $\text{ClCH}_2\text{CH}_2\text{Cl}$.

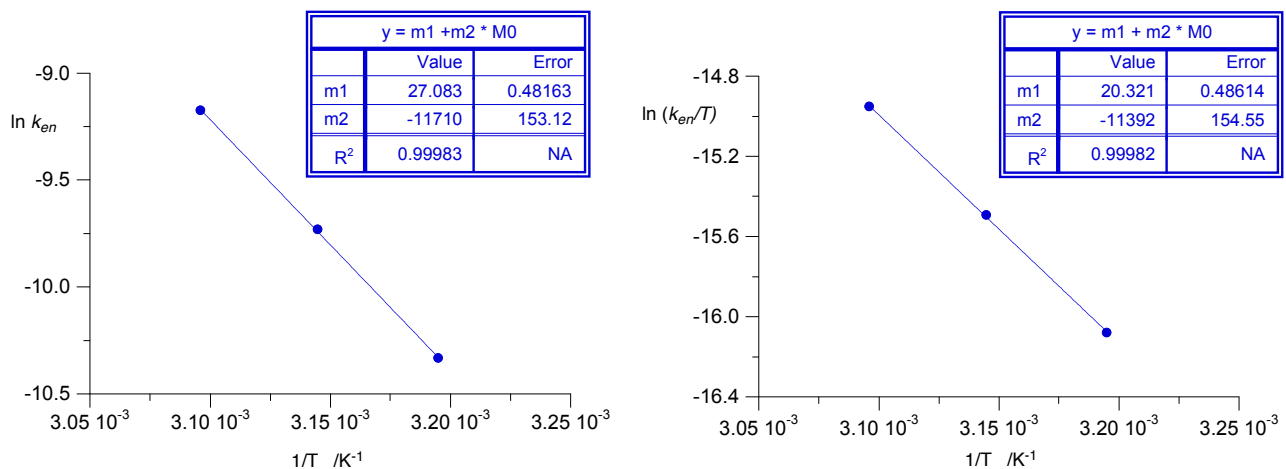


Figure S29. Arrhenius (left) and Eyring (right) plots for enantiomerization of radical **1aA** in $\text{ClCH}_2\text{CH}_2\text{Cl}$.

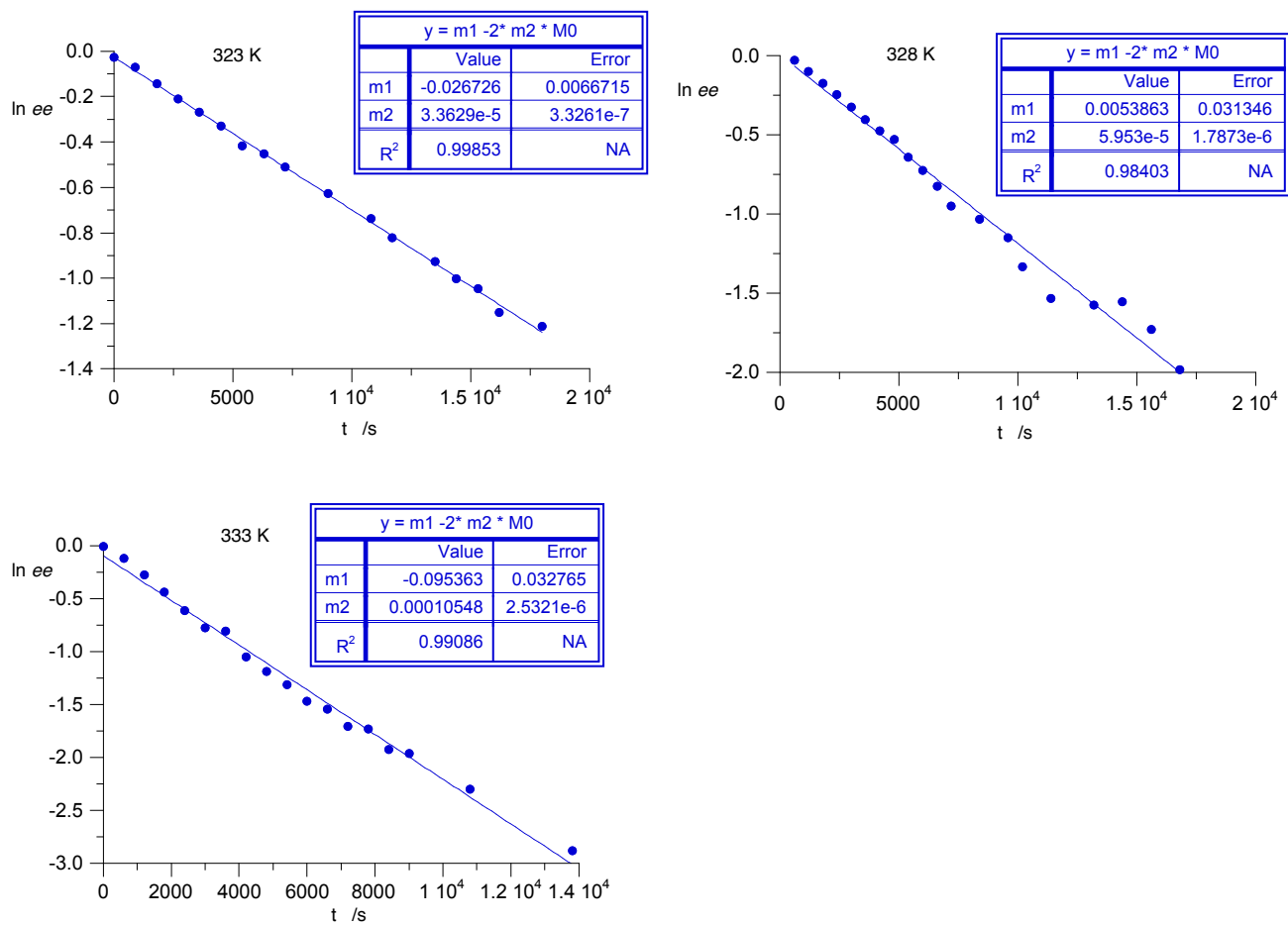


Figure S30. First order kinetics for racemization of radical **1aB** in $\text{ClCH}_2\text{CH}_2\text{Cl}$.

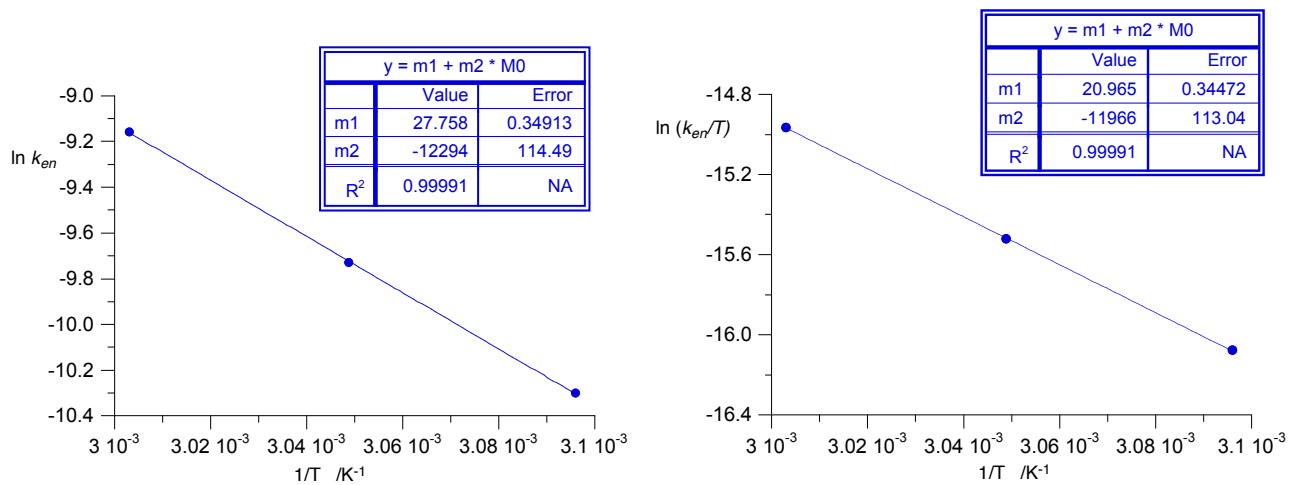


Figure S31. Arrhenius (left) and Eyring (right) plots for enantiomerization of radical **1aB** in $\text{ClCH}_2\text{CH}_2\text{Cl}$.

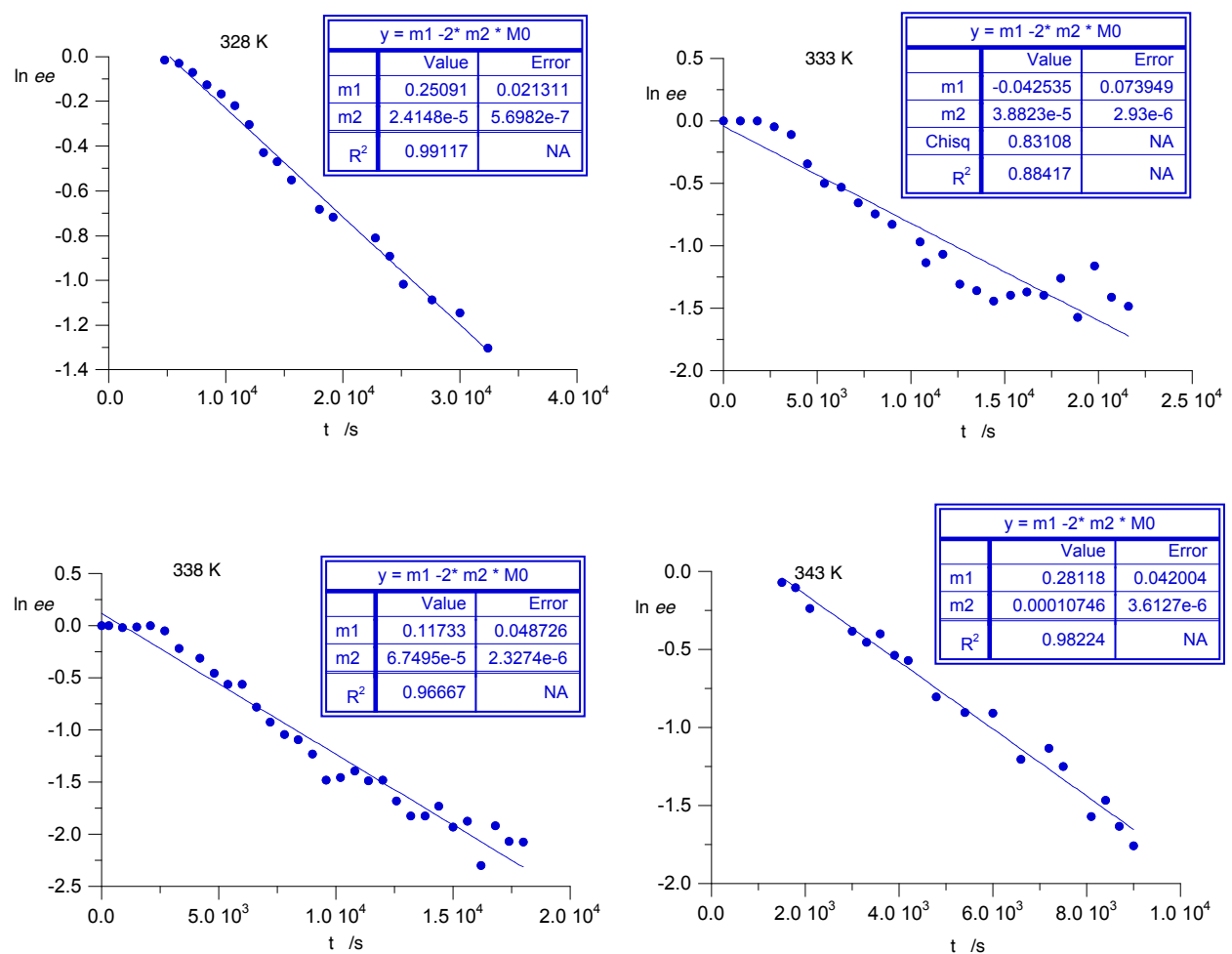


Figure S32. First order kinetics for racemization of radical **1bA** in $\text{ClCH}_2\text{CH}_2\text{Cl}$.

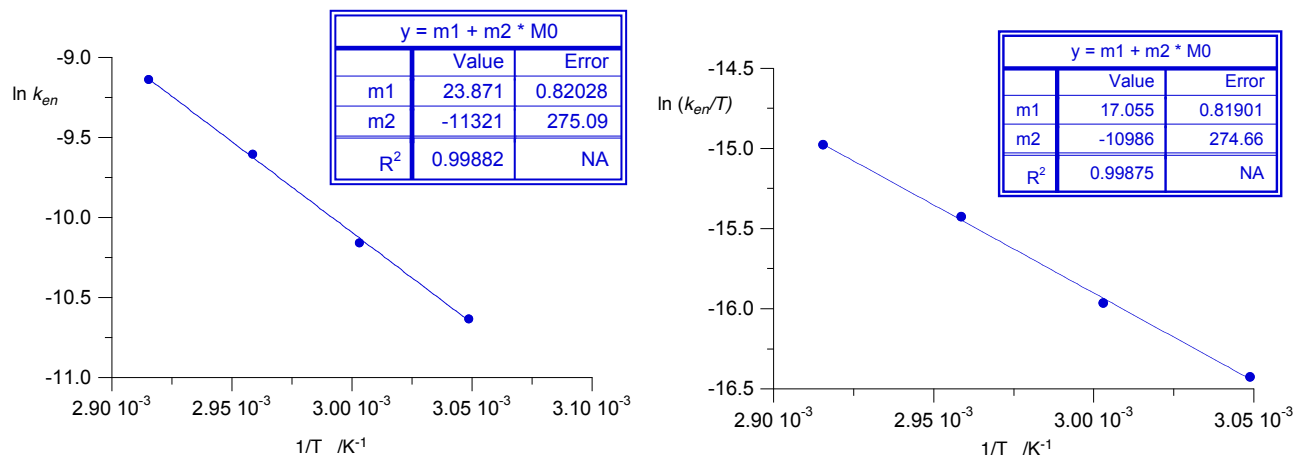


Figure S33. Arrhenius (left) and Eyring (right) plots for enantiomerization of radical **1bA** in $\text{ClCH}_2\text{CH}_2\text{Cl}$.

Table S5. Kinetic data for enantiomerization of radicals **1** in 1,2-dichloroethane obtained by integrations of HPLC signals and Arrhenius and Eyring analyses.

	T /K	$k_{en} \cdot 10^{-4}$ /s ⁻¹	$t_{1/2rac}^a$ /min	Arrhenius analysis (eq 3)		Eyring analysis (eq 4)		
				E_a /kcal mol ⁻¹	lnA	ΔH^\neq /kcal mol ⁻¹	ΔS^\neq /cal(mol K) ⁻¹	ΔG_{298}^\neq /kcal mol ⁻¹
1aA	313	0.326±0.005	177±1.4	23.27±0.3 <i>CI=0.33</i>	27.08±0.48	22.64±0.3	-6.8±1.0 <i>CI=1.1</i>	24.7±0.3
	318	0.59 ±0.01	97±0.1		<i>CI=0.53</i>	<i>CI=0.33</i>	<i>CI=1.1</i>	
	323	1.04±0.02	56±0.1					
1aB	323	0.336±0.003	172±7	24.43±0.2 <i>CI=0.25</i>	27.76±0.35	23.8±0.2	-5.6±0.7 <i>CI=0.75</i>	25.4±0.2
	328	0.595±0.018	97±1.4		<i>CI=0.38</i>	<i>CI=0.25</i>	<i>CI=0.75</i>	
	333	1.055±0.025	55±0.7					
1bA	328	0.241±0.006	239±3	22.49±0.55 <i>CI=0.60</i>	23.9±0.8	21.8±0.55	-13.3±1.6 <i>CI=1.80</i>	25.8±0.55
	333	0.388±0.03	148±5		<i>CI=0.90</i>	<i>CI=0.60</i>	<i>CI=1.80</i>	
	338	0.675±0.02	86±1.3					
	343	1.075±0.04	54±1					

^a Racemization half-time (not enantiomerization) calculated using eq 2 and k_{rac} obtained back from the kinetic fitting line parameters (eq 3). Confidence integral CI calculated at confidence level of 95% according to eq. 6.

Kinetics data for racemization in cyclohexane

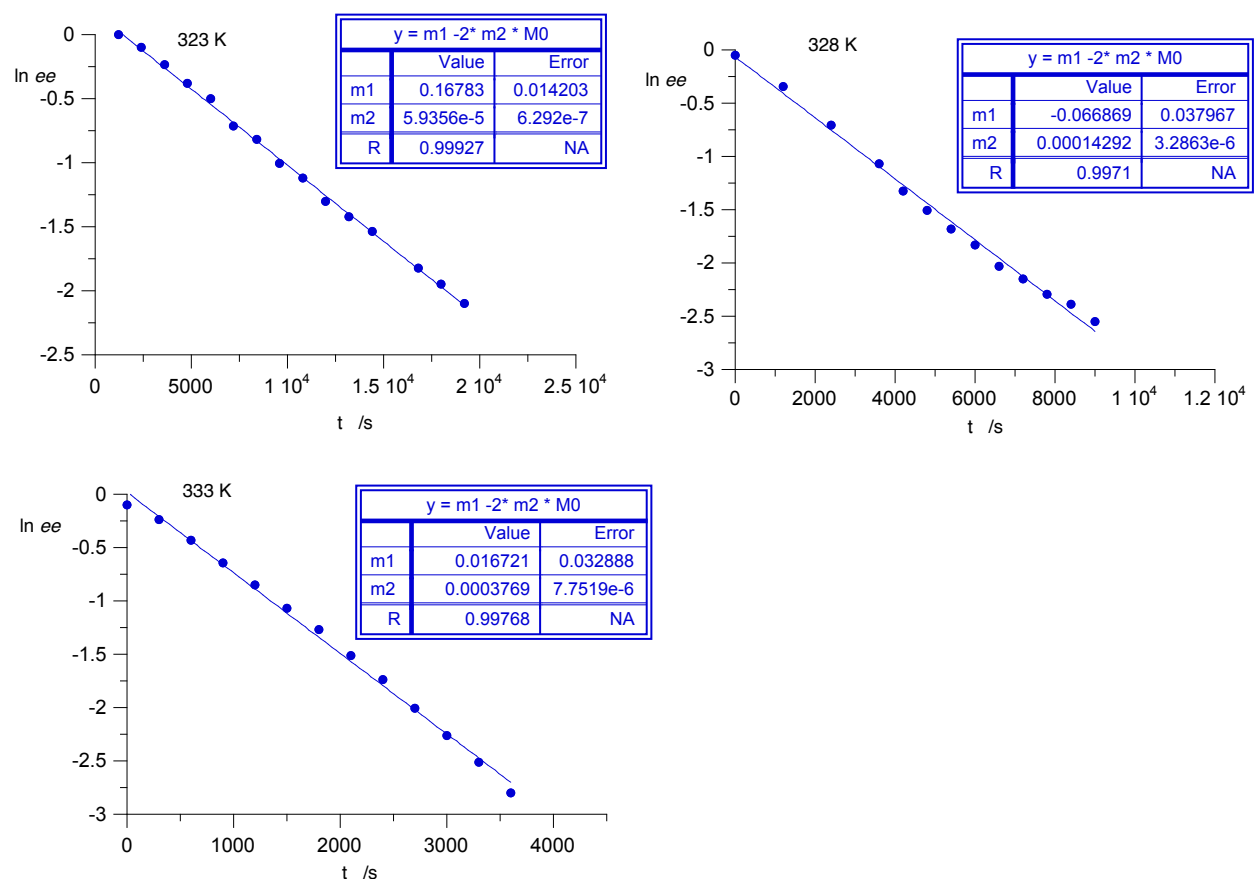


Figure S34. First order kinetics for enantiomerization of radical **1aA** in cyclohexane.

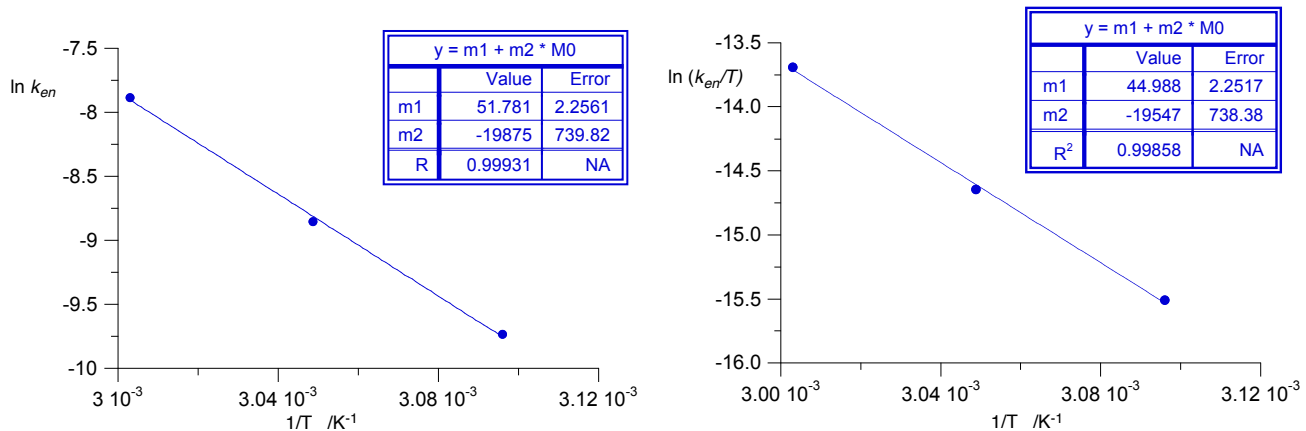


Figure S35. Arrhenius (left) and Eyring (right) plots for enantiomerization of radical **1aA** in cyclohexane.

Table S6. Kinetic data for enantiomerization of radicals **1** in cyclohexane obtained by integrations of HPLC signals and Arrhenius analysis.

	<i>T</i> /K	<i>k_{en}</i> ·10 ⁻⁴ /s ⁻¹	<i>t_{1/2rac}</i> ^a /min	Arrhenius analysis (eq 3)		Eyring analysis (eq 4)		
				<i>E_a</i> /kcal mol ⁻¹	<i>lnA</i>	ΔH^\ddagger /kcal mol ⁻¹	ΔS^\ddagger /cal(mol K) ⁻¹	ΔG_{298}^\ddagger /kcal mol ⁻¹
1aA	323	0.594±0.006	97±0.5	39.5±1.4 <i>CI</i> =1.61	51.8±2.3	38.8±1.5	42.2±4.5	26.3±1.5
	328	1.43±0.03	40±0.5		<i>CI</i> =2.52	<i>CI</i> =1.6	<i>CI</i> =4.9	
	333	3.77±0.08	15.3±0.04					

^a Racemization half-time (not enantiomerization) calculated using eq 2 and *k_{rac}* obtained back from the kinetic fitting line parameters (eq 3). Confidence integral CI calculated at confidence level of 95% according to eq. 6.

13. Computational details

Quantum-mechanical calculations were carried out using Gaussian 09 suite of programs.¹⁴ Geometry optimizations were undertaken at the UB3LYP/Def2SVP level of theory using tight convergence limits. TD-DFT calculations were conducted at the UCAM-B3LYP/Def2SVP // UB3LYP/Def2SVP level of theory in CH₂Cl₂ dielectric medium using the PCM model requested with SCRF(solvent=CH2CL2) keyword, with TD method and 45 or 50 states.

14. Partial output from TD-DFT calculations

s-1aA

state	XX	YY	ZZ	R(length)
1	0.5133	-1.2034	1.8455	0.3851
2	-2.9748	-49.2836	32.5979	-6.5535
3	27.5801	-23.7557	-50.5580	-15.5779
4	-0.7982	-21.0566	12.7433	-3.0372
5	46.8218	12.5288	2.6754	20.6753
6	12.4783	6.7407	-19.8085	-0.1965
7	7.5707	0.7528	-2.1152	2.0694
8	-21.9509	74.0979	-36.0628	5.3614
9	-10.5751	39.4017	-50.9173	-7.3635
10	-62.8119	1.3229	-33.1073	-31.5321
11	-0.8347	2.3420	0.7710	0.7594
12	10.2424	2.1961	-10.9302	0.5028
13	-39.9648	31.0941	-17.9127	-8.9278
14	11.0483	6.3176	-12.6504	1.5718
15	3.3160	38.6209	-48.0856	-2.0496
16	-0.9251	60.3141	0.7409	20.0433
17	-6.8562	15.8191	-0.8499	2.7043
18	1.1328	150.0041	-68.6351	27.5006
19	-184.1382	8.4468	-47.4470	-74.3795

20	-43.1420	42.8513	-37.5679	-12.6195
21	96.8979	89.0340	-2.7284	61.0678
22	-3.2076	-0.2693	-4.9162	-2.7977
23	19.6431	6.1934	-1.2831	8.1845
24	-7.6099	45.6161	-51.6567	-4.5501
25	-19.0597	-3.1200	-30.1299	-17.4366
26	-35.2889	36.2107	2.7422	1.2213
27	-51.6484	74.0560	25.3950	15.9342
28	-0.5165	-11.6171	-2.0013	-4.7116
29	14.2600	402.0719	-25.3534	130.3262
30	-4.0068	109.9438	-23.9800	27.3190
31	124.9404	235.8284	-1.6037	119.7217
32	-106.1655	-0.7834	-79.7770	-62.2420
33	4.8512	1.2238	-17.4784	-3.8011
34	-1.3138	121.6686	1.4840	40.6129
35	-60.9000	138.7981	-307.3033	-76.4684
36	-5.2200	415.6012	-138.4897	90.6305
37	-210.9622	-10.8450	-265.7061	-162.5044
38	3.7744	-5.6019	-0.7066	-0.8447
39	-13.6000	46.3105	-111.6190	-26.3028
40	39.6600	-13.5934	6.0794	10.7153
41	24.3326	8.6651	-10.5060	7.4972
42	-57.2027	22.3557	32.8673	-0.6599
43	-2.1188	1.7784	-4.1190	-1.4865
44	33.4247	84.1474	-3.6830	37.9630
45	22.8363	76.8294	-248.4131	-49.5825
46	10.0825	237.4273	-374.7849	-42.4251
47	147.7654	579.3100	-900.5243	-57.8163
48	472.4565	626.2200	-1968.4808	-289.9348
49	-0.5027	391.9224	-155.9675	78.4841
50	10.1720	77.8371	-6.5763	27.1443

R-1aA

Rotatory Strengths (R) in cgs (10**-40 erg-esu-cm/Gauss)				
state	XX	YY	ZZ	R(length)
1	-0.5133	1.2030	-1.8451	-0.3851
2	2.9752	49.2845	-32.5996	6.5534
3	-27.5808	23.7522	50.5587	15.5767
4	0.7983	21.0591	-12.7434	3.0380
5	-46.8212	-12.5287	-2.6760	-20.6753
6	-12.4784	-6.7410	19.8089	0.1965
7	-7.5704	-0.7529	2.1152	-2.0694
8	21.9508	-74.0971	36.0623	-5.3613
9	10.5767	-39.4014	50.9176	7.3643
10	62.8097	-1.3225	33.1057	31.5310
11	0.8346	-2.3418	-0.7710	-0.7594
12	-10.2423	-2.1967	10.9311	-0.5026
13	39.9649	-31.0932	17.9128	8.9282
14	-11.0481	-6.3177	12.6502	-1.5719
15	-3.3154	-38.6173	48.0867	2.0513
16	0.9255	-60.3166	-0.7414	-20.0442
17	6.8531	-15.8194	0.8488	-2.7059
18	-1.1344	-150.0039	68.6362	-27.5007
19	184.1480	-8.4464	47.4498	74.3838
20	43.1360	-42.8502	37.5658	12.6172
21	-96.8975	-89.0363	2.7282	-61.0686
22	3.2076	0.2690	4.9162	2.7976
23	-19.6425	-6.1930	1.2831	-8.1842

24	7.6106	-45.6170	51.6572	4.5503
25	19.0604	3.1200	30.1296	17.4367
26	35.2887	-36.2102	-2.7421	-1.2212
27	51.6451	-74.0545	-25.3963	-15.9352
28	0.5181	11.6170	2.0018	4.7123
29	-14.2640	-402.0811	25.3534	-130.3306
30	4.0050	-109.9462	23.9803	-27.3203
31	-124.9366	-235.8197	1.6040	-119.7175
32	106.1681	0.7833	79.7841	62.2451
33	-4.8484	-1.2242	17.4764	3.8013
34	1.3142	-121.6772	-1.4801	-40.6144
35	60.8996	-138.7788	307.2872	76.4693
36	5.2283	-415.6151	138.4986	-90.6294
37	210.9662	10.8491	265.7013	162.5055
38	-3.7864	5.5997	0.7021	0.8384
39	13.6011	-46.3058	111.6204	26.3052
40	-39.6585	13.5933	-6.0857	-10.7170
41	-24.3351	-8.6670	10.4988	-7.5011
42	57.2011	-22.3505	-32.8604	0.6634
43	2.1194	-1.7787	4.1174	1.4860
44	-33.4268	-84.1461	3.6821	-37.9636
45	-22.8379	-76.8306	248.4209	49.5842
46	-10.0820	-237.4119	374.7673	42.4245
47	-147.7363	-579.2336	900.3707	57.8003
48	-472.4845	-626.3002	1968.6572	289.9575
49	0.5019	-391.9272	155.9785	-78.4823
50	-10.1726	-77.8424	6.5767	-27.1461

S-1aB

Rotatory Strengths (R) in cgs (10**-40 erg-esu-cm/Gauss)

state	XX	YY	ZZ	R(length)
1	0.0546	-3.0072	4.3065	0.4513
2	-1.4786	-76.1054	53.6402	-7.9813
3	58.5558	-4.2650	-111.5007	-19.0700
4	-5.3281	-18.8137	18.7492	-1.7975
5	66.5499	-8.6811	1.3524	19.7404
6	27.0422	2.6922	-31.6728	-0.6461
7	19.7764	-2.1968	-7.6780	3.3005
8	-46.2331	61.8432	1.7019	5.7707
9	45.9842	-0.8850	-12.0496	11.0165
10	-137.1471	0.1650	-5.0095	-47.3305
11	-4.4897	0.8733	5.3469	0.5768
12	2.3732	5.0071	-13.4971	-2.0389
13	-49.8412	12.2761	14.9434	-7.5406
14	12.0320	10.7975	-18.4343	1.4651
15	-0.0093	13.1174	-57.2312	-14.7077
16	20.0886	16.3952	99.1225	45.2021
17	-277.4652	-6.1047	3.3017	-93.4227
18	89.2772	34.0318	33.5792	52.2961
19	-47.4206	3.9994	1.8246	-13.8655
20	-1.3688	3.6759	5.1480	2.4850
21	16.1298	120.9571	39.5482	58.8784
22	-1.7809	-4.3524	-0.5135	-2.2156
23	-1.4978	-0.0296	-8.6233	-3.3836
24	2.2910	22.6382	11.3637	12.0976
25	-73.9452	40.7699	-8.7308	-13.9687
26	0.3309	-0.5641	-1.0216	-0.4183
27	-19.6832	-73.6900	62.2607	-10.3708

28	-65.3587	13.1947	69.4030	5.7463
29	-443.9611	935.1155	317.0327	269.3957
30	0.1916	2.2157	-18.9283	-5.5070
31	13.4299	65.6174	13.5083	30.8519
32	-90.5256	1.8248	-38.5920	-42.4309
33	-62.6578	2.0417	-27.8354	-29.4838
34	1.8240	22.7607	1.2872	8.6240
35	-240.7230	224.0092	-93.2160	-36.6433
36	-123.1505	431.6988	57.7491	122.0991
37	-515.8913	53.3844	-264.3819	-242.2963
38	55.3619	15.6121	0.5457	23.8399
39	1.3545	2.4180	0.4196	1.3974
40	14.9498	-61.1141	128.3191	27.3850
41	-19.2071	0.5615	-48.1483	-22.2646
42	-60.5271	-7.4427	98.5767	10.2023
43	-0.8285	0.6181	0.1896	-0.0069
44	-10.2632	20.2313	-48.7297	-12.9205
45	45.9794	3.5248	8.8865	19.4636
46	-10.7859	40.5000	-32.1881	-0.8247
47	-28.3063	229.0530	-119.7671	26.9932
48	-183.0232	1275.6874	-2371.0599	-426.1319
49	93.5066	-5.9965	157.0231	81.5110
50	8.7880	73.0594	5.9058	29.2511

R-1aB

Rotatory Strengths (R) in cgs (10**-40 erg-esu-cm/Gauss)

state	XX	YY	ZZ	R(length)
1	-0.0546	3.0072	-4.3064	-0.4513
2	1.4786	76.1054	-53.6402	7.9813
3	-58.5558	4.2650	111.5008	19.0700
4	5.3281	18.8137	-18.7492	1.7975
5	-66.5499	8.6811	-1.3524	-19.7404
6	-27.0422	-2.6922	31.6728	0.6461
7	-19.7764	2.1968	7.6780	-3.3005
8	46.2331	-61.8432	-1.7020	-5.7707
9	-45.9842	0.8850	12.0496	-11.0165
10	137.1472	-0.1650	5.0095	47.3306
11	4.4897	-0.8733	-5.3469	-0.5768
12	-2.3731	-5.0071	13.4971	2.0389
13	49.8413	-12.2761	-14.9434	7.5406
14	-12.0320	-10.7975	18.4343	-1.4651
15	0.0093	-13.1174	57.2313	14.7077
16	-20.0885	-16.3951	-99.1227	-45.2021
17	277.4647	6.1047	-3.3019	93.4225
18	-89.2767	-34.0318	-33.5790	-52.2958
19	47.4206	-3.9994	-1.8246	13.8656
20	1.3688	-3.6759	-5.1480	-2.4850
21	-16.1299	-120.9571	-39.5483	-58.8784
22	1.7809	4.3524	0.5135	2.2156
23	1.4978	0.0296	8.6233	3.3836
24	-2.2910	-22.6381	-11.3637	-12.0976
25	73.9455	-40.7700	8.7307	13.9687
26	-0.3311	0.5642	1.0216	0.4182
27	19.6833	73.6900	-62.2608	10.3708
28	65.3587	-13.1948	-69.4030	-5.7463
29	443.9613	-935.1153	-317.0331	-269.3957
30	-0.1916	-2.2158	18.9283	5.5070
31	-13.4298	-65.6170	-13.5081	-30.8516

32	90.5258	-1.8248	38.5920	42.4310
33	62.6573	-2.0417	27.8353	29.4836
34	-1.8241	-22.7606	-1.2872	-8.6240
35	240.7233	-224.0090	93.2159	36.6434
36	123.1506	-431.6985	-57.7493	-122.0991
37	515.8912	-53.3844	264.3814	242.2961
38	-55.3619	-15.6122	-0.5457	-23.8399
39	-1.3544	-2.4180	-0.4195	-1.3973
40	-14.9498	61.1142	-128.3191	-27.3849
41	19.2071	-0.5615	48.1483	22.2646
42	60.5270	7.4428	-98.5766	-10.2023
43	0.8285	-0.6181	-0.1897	0.0069
44	10.2631	-20.2314	48.7298	12.9205
45	-45.9794	-3.5248	-8.8864	-19.4635
46	10.7859	-40.5000	32.1882	0.8247
47	28.3065	-229.0540	119.7679	-26.9932
48	183.0231	-1275.6840	2371.0566	426.1319
49	-93.5065	5.9968	-157.0231	-81.5109
50	-8.7882	-73.0592	-5.9058	-29.2511

S-1bA

Rotatory Strengths (R) in cgs (10**-40 erg-esu-cm/Gauss)

state	XX	YY	ZZ	R(length)
1	0.6956	-0.0591	0.9812	0.5392
2	64.0358	-91.2870	39.9864	4.2451
3	-13.3077	-30.6084	2.2864	-13.8766
4	9.5089	30.5653	-68.3024	-9.4094
5	65.0425	42.0359	-42.2013	21.6257
6	8.4335	4.7727	-7.8168	1.7965
7	-0.2840	-1.0777	4.5384	1.0589
8	48.6257	67.8354	-61.5200	18.3137
9	-14.8017	13.6878	-89.3094	-30.1411
10	-19.4425	53.0441	-142.5855	-36.3279
11	-48.7844	14.8050	-14.5124	-16.1639
12	3.4696	13.0231	1.7163	6.0696
13	-27.5194	70.2914	-51.6695	-2.9658
14	7.8139	49.6980	-6.3276	17.0614
15	20.8728	140.8170	-56.6962	34.9979
16	-1.4970	36.9350	-11.6923	7.9152
17	-46.2623	80.1299	15.5619	16.4765
18	3.0065	-0.3348	-31.5917	-9.6400
19	17.6682	-0.2659	-63.8067	-15.4681
20	0.2381	1.0491	-11.8322	-3.5150
21	-5.0215	9.2628	-26.6699	-7.4762
22	9.8461	1.7299	2.1918	4.5893
23	-13.3514	54.9690	14.0212	18.5463
24	6.5579	-3.4598	4.0219	2.3733
25	-0.1711	0.9605	-3.8505	-1.0204
26	6.7790	8.9604	-22.0464	-2.1023
27	-1.6324	16.4612	-26.1871	-3.7861
28	1.2807	92.1262	-94.8960	-0.4963
29	-17.2258	64.8689	-292.4797	-81.6122
30	0.6365	2.9409	-7.9778	-1.4668
31	0.0250	3.2474	-0.0270	1.0818
32	1.9083	10.0315	-25.7797	-4.6133
33	-35.4518	-0.7632	-0.4476	-12.2209
34	-31.2817	109.4601	-538.9196	-153.5804
35	2.1542	221.2694	3.2131	75.5456

36	167.4442	585.3511	-2131.3942	-459.5330
37	82.9637	29.9098	-462.0832	-116.4032
38	-140.5379	1307.5050	346.7345	504.5672
39	3.1783	15.1403	-265.1027	-82.2614
40	380.0752	369.9128	-119.0886	210.2998
41	-2.9510	156.9990	-42.9014	37.0489
42	-5.4210	65.7937	12.2261	24.1996
43	-0.2793	1.4703	-13.9138	-4.2410
44	2.0671	-2.1535	-199.2690	-66.4518
45	-71.3845	151.0469	-144.2315	-21.5230

R-1bA

Rotatory Strengths (R) in cgs (10^{**-40} erg-esu-cm/Gauss)

state	XX	YY	ZZ	R(length)
1	-0.6956	0.0591	-0.9811	-0.5392
2	-64.0307	91.2829	-39.9857	-4.2445
3	13.3052	30.6093	-2.2898	13.8749
4	-9.5088	-30.5661	68.3064	9.4105
5	-65.0421	-42.0342	42.1984	-21.6260
6	-8.4324	-4.7721	7.8160	-1.7962
7	0.2841	1.0798	-4.5383	-1.0581
8	-48.6260	-67.8409	61.5263	-18.3135
9	14.7999	-13.6841	89.2943	30.1367
10	19.4419	-53.0458	142.5889	36.3283
11	48.7869	-14.8052	14.5153	16.1656
12	-3.4691	-13.0214	-1.7154	-6.0686
13	27.5178	-70.2890	51.6706	2.9665
14	-7.8128	-49.7037	6.3249	-17.0639
15	-20.8732	-140.8071	56.6929	-34.9958
16	1.4973	-36.9425	11.6943	-7.9170
17	46.2630	-80.1230	-15.5632	-16.4744
18	-3.0044	0.3347	31.5803	9.6369
19	-17.6692	0.2657	63.8189	15.4718
20	-0.2385	-1.0483	11.8365	3.5166
21	5.0213	-9.2618	26.6634	7.4743
22	-9.8459	-1.7320	-2.1891	-4.5890
23	13.3514	-54.9672	-14.0238	-18.5465
24	-6.5581	3.4602	-4.0213	-2.3731
25	0.1709	-0.9600	3.8501	1.0203
26	-6.7781	-8.9591	22.0446	2.1025
27	1.6326	-16.4570	26.1825	3.7861
28	-1.2809	-92.1284	94.8974	0.4960
29	17.2246	-64.8653	292.4650	81.6081
30	-0.6365	-2.9397	7.9763	1.4667
31	-0.0248	-3.2497	0.0263	-1.0827
32	-1.9085	-10.0301	25.7786	4.6133
33	35.4393	0.7616	0.4439	12.2149
34	31.2923	-109.4610	538.9297	153.5870
35	-2.1551	-221.2800	-3.2107	-75.5486
36	-167.4546	-585.3752	2131.4146	459.5283
37	-82.9714	-29.8705	462.1553	116.4378
38	140.5234	-1307.4828	-346.7073	-504.5556
39	-3.1565	-15.1703	265.0356	82.2363
40	-380.0530	-369.9316	119.0405	-210.3147
41	2.9518	-156.9866	42.9106	-37.0414
42	5.4195	-65.7863	-12.2245	-24.1971
43	0.2776	-1.4700	13.9379	4.2485
44	-2.0662	2.1523	199.2399	66.4420

15. Archive for DFT calculations

S-1aA

```
1\1\GINC-LOCALHOST\FOpt\UB3LYP\def2SVP\C29H20N3(2)\PIOTR\23-Mar-2021\0
  \#P UB3LYP/Def2SVP FOpt(tight) Geom=(NoDistance,NoAngle) fcheck\naphthalene-1-(3-Ph-benzotrizin-1-yl)-8-Ph, S isomer\0,2\C,2.3850213091,-2.0653649206,-4.4073410291\C,1.514347509,-1.6268161742,-3.4165419869\C,1.8299647371,-1.9148564336,-2.0376937433\C,2.9639991794,-2.7681093329,-1.7629014183\C,3.8005608068,-3.2043597351,-2.8270929334\C,3.5356632957,-2.8329287421,-4.1238061288\C,1.1237354112,-1.4122174345,-0.8906538844\C,3.2531727569,-3.1739771077,-0.4308997631\C,2.4833435044,-2.7455941589,0.6262176834\C,1.4285242294,-1.8406263579,0.3895179661\H,2.1355746495,-1.8465894929,-5.4480755584\H,4.6582706598,-3.8390233771,-2.5902228073\H,4.1839002653,-3.1592493975,-4.9406569167\H,4.1062245125,-3.836727857,-0.264315606\H,2.7033890384,-3.068328535,1.6463096849\H,0.8451259006,-1.4416115275,1.2209460891\C,0.3999826696,0.9266247706,-1.2594390699\C,1.6924260035,1.3894224777,-1.5526391971\C,-0.7002573755,1.8352197308,-1.2037717732\C,-2.0851815791,0.126530214,-0.5320083055\C,1.8943721183,2.7424123252,-1.825320852\C,-0.4598557965,3.1967685037,-1.4921770585\C,0.8184728126,3.6450637968,-1.8031114501\H,2.5325498625,0.6956830657,-1.5683016506\H,2.9020359192,3.0972704032,-2.0545502196\H,-1.3142699633,3.8747322047,-1.4490665468\H,0.9888748451,4.7021116178,-2.0211472144\C,0.2550972909,-0.9693095904,-3.8842037366\C,-0.9985241705,-1.5514701966,-3.6256887456\C,-2.1644146309,-1.0015737837,-4.1624576619\C,-0.8599195264,0.7248108504,-5.2371763813\N,-1.1236205108,-0.8011826891,-0.5671944939\N,-1.9513439615,1.4147633311,-0.8548733044\C,-2.0999396016,0.1390389291,-4.9689195938\C,0.3071837868,0.1727096466,-4.7029590691\H,-0.7989316606,1.6196515641,-5.86188821\H,-1.0595909489,-2.4437665404,-2.9992415563\H,-3.1292581805,-1.4672442319,-3.9468722653\H,-3.0141456344,0.5704217201,-5.3842508095\H,1.27339169,0.6391215738,-4.9095421444\C,-3.4270509759,-0.3478345373,-0.0875462573\C,-4.495087125,0.5617480875,-0.006701898\C,-3.6489774725,-1.6932651177,0.2558269357\C,-5.7576696311,0.1346643701,0.4079371499\C,-4.9126944497,-2.1165741016,0.6699221891\C,-5.9716406777,-1.2051662929,0.7475771679\H,-4.3106351682,1.6025426429,-0.2752755018\H,-2.8186955236,-2.3976202792,0.1935066798\H,-6.5803870743,0.8522210869,0.4668105906\H,-5.0731014199,-3.1651515387,0.9345230763\H,-6.9607544123,-1.5389258995,1.0724311329\N,0.0997681568,-0.4093295091,-0.9916089734\Version=ES64L-G09RevD.01\State=2-A\HF=-1280.4476115\S2=0.767213\S2-1=0.\S2A=0.75017\RMSD=3.207e-09\RMSF=1.031e-06\Dipole=1.1545611,-0.3164027,-0.2473488\Quadrupole=4.8123307,-0.6284905,-4.1838402,-2.5024791,-0.2509008,-4.964137\PG=C01 [X(C29H20N3)]\@\@
```

R-1aA

```
1\1\GINC-LOCALHOST\FOpt\UB3LYP\def2SVP\C29H20N3(2)\PIOTR\23-Mar-2021\0
  \#P UB3LYP/Def2SVP FOpt(tight) Geom=(NoDistance,NoAngle) fcheck\naphthalene-1-(3-Ph-benzodiazzen-1-yl)-8-Ph\0,2\C,3.7871370394,0.2101342274,1.6362607251\C,2.5464759932,0.0154631392,1.0404888235\C,2.4037868211,-1.0354680197,0.0612097592\C,3.5225959468,-1.926304713,-0.1491728061\C,4.7579979433,-1.6856654341,0.5130421521\C,4.8990766767,-0.6169572342,1.3660112109\C,1.2425300658,-1.2752400968,-0.7518684806\C,3.3985172076,-3.0443885934,-1.0192710668\C,2.2279526966,-3.2895402893,-1.6999520586\C,1.1560911674,-2.3817950524,-1.5785094114\H,3.8843485816,1.0048529685,2.3793535721\H,5.5914744069,-2.3677718949,0.3269799436\H,5.8510163968,-0.4255389474,1.8671213205\H,4.2590396772,-3.7079682644,-1.1369533266\H,2.1342626645,-4.1554061644,-2.3592422096\H,0.2418377019,-2.5250547108,-2.1568315401\C,0.2034005541,0.8602636579,-1.4517512887\C,1.3797823259,1.36267364,-2.0299101341\C,-1.0149226083,1.6014273975,-1.526162
```

5394\c, -2.1367728131, -0.1287912949, -0.5079787892\c, 1.3632826434, 2.6115
 691106, -2.6509637815\c, -0.9927756342, 2.8651446247, -2.1564913438\c, 0.18
 03125195, 3.3666618382, -2.707960218\h, 2.3004747389, 0.7810674384, -1.9926
 604954\h, 2.2819954403, 2.9988130858, -3.0980269527\h, -1.932778361, 3.4183
 978282, -2.1991809319\h, 0.1806703229, 4.3448772381, -3.1948084246\c, 1.425
 8808671, 0.8648213904, 1.5499900439\c, 0.3233587515, 0.284669826, 2.2020466
 184\c, -0.6641570796, 1.0840848262, 2.7813183524\c, 0.5247079106, 3.0671586
 628, 2.0804973497\n, -1.0474635905, -0.8926934681, -0.3801330591\n, -2.1829
 550272, 1.0993242554, -1.0288455225\c, -0.5681518353, 2.4779171226, 2.72173
 99923\c, 1.5147218197, 2.267409109, 1.5037761086\h, 0.606622457, 4.15563318
 34, 2.0235984086\h, 0.2401923089, -0.8027558126, 2.2563307169\h, -1.5147739
 517, 0.6135786887, 3.2806417545\h, -1.3445192729, 3.1016620292, 3.171806108
 1\h, 2.3631999902, 2.733201754, 0.9969264085\c, -3.4095110095, -0.727386823
 , -0.0130018297\c, -4.6078036544, -0.0012444906, -0.1197203865\c, -3.438063
 0623, -2.0108446819, 0.5608106068\c, -5.8082964213, -0.5467891188, 0.338142
 9128\c, -4.6402209404, -2.5529742998, 1.0174920576\c, -5.8295235197, -1.823
 7970068, 0.908305496\h, -4.5730663175, 0.992897304, -0.5668031076\h, -2.507
 3119942, -2.573424019, 0.6418967515\h, -6.7338485499, 0.0282465276, 0.24923
 3076\h, -4.6500016051, -3.5519197074, 1.4616441457\h, -6.7701843939, -2.250
 5290907, 1.2665350318\n, 0.1286780054, -0.3686366452, -0.7953547428\\Version=ES64L-G09RevD.01\\State=2-A\\HF=-1280.4476115\\S2=0.767213\\S2-1=0.\\S2A=0.75017\\RMSD=4.801e-09\\RMSF=1.045e-06\\Dipole=1.2060089,-0.151047,-0.1305194\\Quadrupole=3.7838909,2.9959064,-6.7797973,-1.8424531,-3.6132424,0.646579\\PG=C01 [X(C29H20N3)]\\

S-1aB

1\1\GINC-LOCALHOST\FOpt\UB3LYP\def2SVP\C33H28N3(2)\PIOTR\24-Mar-2021\0
 \\#P UB3LYP/Def2SVP FOpt(tight) Geom=(NoDistance,NoAngle) fcheck\\naphthalene-1-(3-Ph-benzoTriazin-1-yl)-8-Ph-Bu opt in vac isomer S\\0,2\c
 , 3.7912198874, 0.1821963189, -1.6842824909\c, 2.5552331524, -0.0124334448,
 -1.0787750873\c, 2.4312366202, -1.0360488312, -0.0680710032\c, 3.560292298
 4, -1.9094733661, 0.1587130718\c, 4.7893925338, -1.6723622186, -0.516172676
 1\c, 4.9142519163, -0.6237212957, -1.3965207984\c, 1.2787896717, -1.2634224
 164, 0.7621698323\c, 3.45198016, -3.0067270312, 1.0573185743\c, 2.288368319
 8, -3.2449552176, 1.7522054492\c, 1.2080049357, -2.3490260095, 1.6175241633
 \h, 3.8751916878, 0.957224549, -2.4495441346\h, 5.6312962932, -2.340492969,
 -0.3176806612\h, 5.8618227815, -0.4344638837, -1.9067365287\h, 4.319228535
 5, -3.6595739517, 1.1855141862\h, 2.2072289398, -4.0947839601, 2.4336801493
 \h, 0.3004404424, -2.4835229548, 2.2083096255\c, 0.2441672541, 0.896071433,
 1.3920274747\c, 1.4225854727, 1.4141656831, 1.952128441\c, -0.9671887045, 1.
 6513763617, 1.4252988623\c, -2.1035482441, -0.1238357666, 0.5050085858\c,
 1.4156325871, 2.6918267897, 2.5114623464\c, -0.9355122064, 2.9441265858, 1.
 9928749916\c, 0.2401354665, 3.4604821733, 2.5249596155\h, 2.337796849, 0.82
 2865691, 1.9472986904\h, 2.3359242052, 3.0913068434, 2.9442645897\h, -1.870
 0411107, 3.5079880323, 2.0062720552\h, 0.2481563125, 4.461260159, 2.9634934
 112\c, 1.4175431365, 0.801601415, -1.6025075463\c, 0.3121153647, 0.19283805
 24, -2.2136560741\c, -0.7092258659, 0.9558983153, -2.7851970127\c, 0.445607
 5981, 2.9624267645, -2.1733630048\n, -1.0206779325, -0.9017917263, 0.419326
 8713\n, -2.1380677293, 1.1361243351, 0.9465704792\c, -0.6760289441, 2.35942
 68036, -2.7723834462\c, 1.4703811083, 2.2062243396, -1.606174372\h, 0.52300
 60297, 4.0513973381, -2.1327320675\h, 0.2430089591, -0.8967546597, -2.24333
 61944\h, -1.5474735237, 0.4280981971, -3.2398233266\h, 2.3178062805, 2.7127
 402476, -1.1377727293\c, -3.3824601216, -0.7423873525, 0.0514761597\c, -4.5
 817051339, -0.0159685747, 0.1483549844\c, -3.4158879624, -2.0471954556, -0.
 4719402417\c, -5.7868641457, -0.5811660764, -0.2727333294\c, -4.6226179627
 , -2.6090116407, -0.8912267949\c, -5.812242706, -1.8787101857, -0.794154129
 5\h, -4.5456444512, 0.9926305933, 0.5615793501\h, -2.4846711248, -2.6100882
 881, -0.5446914654\h, -6.7129646345, -0.0058800453, -0.1916128933\h, -4.635

6092022,-3.6239876777,-1.2972637025\H,-6.756493667,-2.3205780239,-1.12
 33886798\N,0.1608491553,-0.3616361384,0.7943315738\C,-1.8074555867,3.2
 297266969,-3.3513252107\C,-2.9240662561,2.3828812588,-3.9885250425\C,-
 2.4287492055,4.0674728547,-2.2088042856\C,-1.2371827189,4.1730040759,-
 4.4351695941\H,-2.5483979679,1.7663555507,-4.8204386496\H,-3.403031317
 5,1.7157037656,-3.2554214007\H,-3.7065537099,3.0437503788,-4.393972759
 8\H,-1.6912166312,4.7447602042,-1.751363906\H,-3.2586035521,4.68522825
 61,-2.590780717\H,-2.8206085959,3.4143159987,-1.4133339404\H,-2.036838
 0327,4.8071135592,-4.8524407284\H,-0.4600315524,4.8411375575,-4.033579
 3188\H,-0.7911868055,3.5996811831,-5.2637519499\Version=ES64L-G09RevD
 .01\State=2-A\HF=-1437.5884562\S2=0.766954\S2-1=0.\S2A=0.750166\RMSD=3
 .005e-09\RMSF=9.176e-07\Dipole=1.0716333,-0.0970197,0.1289794\Quadrupo
 le=4.6898285,2.5197957,-7.2096242,-2.9221643,4.8636504,-1.2265251\PG=C
 01 [X(C33H28N3)]\\

R-1aB

1\1\GINC-LOCALHOST\FOpt\UB3LYP\def2SVP\C33H28N3(2)\PIOTR\24-Mar-2021\0
 \\#P UB3LYP/Def2SVP FOpt(tight) Geom=(NoDistance,NoAngle) fcheck\naph
 thalene-1-(3-Ph-benzoTriazin-1-yl)-8-Ph-Bu opt at Def2SVP in vac\0,2\
 C,3.791176666,0.1820582953,1.6843979278\C,2.5552057995,-0.0125148173,1
 .0788399788\C,2.431217778,-1.0360853685,0.0680894788\C,3.5602587823,-1
 .9095296188,-0.1586916572\C,4.7893418675,-1.672477825,0.5162461601\C,4
 .9141978847,-0.6238763245,1.3966417126\C,1.2787936076,-1.2633950813,-0
 .7622004492\C,3.4519493485,-3.006743535,-1.0573460186\C,2.2883553044,-
 3.2449131814,-1.7522827642\C,1.2080103611,-2.3489616602,-1.6176018694\
 H,3.8751420167,0.9570528589,2.4496943563\H,5.6312352989,-2.3406220399,
 0.3177556633\H,5.8617560558,-0.4346642535,1.9068978244\H,4.3191853349,
 -3.6596075089,-1.1855386113\H,2.2072175064,-4.0947118092,-2.43379522\H
 ,0.3004627785,-2.4834108889,-2.2084241838\C,0.2442488491,0.8961513764,
 -1.3920051877\C,1.4226998626,1.4142381241,-1.9520440454\C,-0.967086430
 9,1.6514889768,-1.4252876259\C,-2.1035237663,-0.1237315451,-0.50510952
 48\C,1.4157993807,2.6919223266,-2.5113258125\C,-0.9353568576,2.9442616
 373,-1.9928096696\C,0.2403226047,3.4606086385,-2.5248323609\H,2.337895
 7822,0.8229142973,-1.9472067903\H,2.3361163226,3.0913963395,-2.9440797
 543\H,-1.869870728,3.5081477847,-2.0062160476\H,0.2483845232,4.4614043
 753,-2.9633248735\C,1.4175185802,0.8015275485,1.6025667993\C,0.3120542
 154,0.1927672076,2.2136521162\C,-0.7092871601,0.9558299678,2.785189440
 2\C,0.4456187022,2.9623541604,2.173478114\N,-1.0206765116,-0.901718997
 9,-0.4194221598\N,-2.1379953965,1.136247571,-0.9466209725\C,-0.6760538
 95,2.3593581497,2.7724350458\C,1.470392364,2.2061489595,1.6062934725\H
 ,0.5230463994,4.0513244391,2.1328948817\H,0.2429189359,-0.896824957,2.
 2432848667\H,-1.5475639503,0.4280324942,3.2397651364\H,2.317846637,2.7
 126625159,1.1379419667\C,-3.3824673467,-0.74226866,-0.0516467621\C,-4.
 5816902928,-0.0158150261,-0.1485375911\C,-3.4159470059,-2.047097269,0.
 4717152249\C,-5.7868785022,-0.5809986783,0.272485752\C,-4.6227060466,-
 2.6088994697,0.8909369093\C,-5.8123086028,-1.8785634133,0.7938527017\H
 ,-4.545589285,0.9928000968,-0.5617195325\H,-2.4847471939,-2.6100170557
 ,0.5444758357\H,-6.7129613557,-0.0056854811,0.1913566007\H,-4.63573754
 22,-3.6238917382,1.2969319348\H,-6.7565823856,-2.3204203657,1.12303639
 09\N,0.160877524,-0.3615785525,-0.7943637531\C,-1.8074781209,3.2296630
 442,3.351373996\C,-2.4287109404,4.0674725763,2.2088664522\C,-2.9241324
 325,2.382819829,3.9885003012\C,-1.237218312,4.1728808458,4.4352771425\
 H,-1.6911452563,4.7447600518,1.7514796319\H,-2.8205596461,3.4143587989
 ,1.4133554569\H,-3.2585626235,4.6852333491,2.590839981\H,-2.5485085584
 ,1.7662499214,4.8204012073\H,-3.7066168391,3.0436922286,4.3939485538\H
 ,-3.4030894561,1.7156850746,3.2553524952\H,-2.0368716946,4.8069936463,
 4.8525469342\H,-0.7912657805,3.5995121289,5.2638511454\H,-0.460036058,
 4.8410109057,4.0337413378\Version=ES64L-G09RevD.01\State=2-A\HF=-1437

```
.5884562\S2=0.766954\S2-1=0.\S2A=0.750166\RMSD=2.828e-09\RMSF=9.175e-0
7\Di pole=1.071635,-0.0970422,-0.1289462\Quadrupole=4.6900142,2.5198432
,-7.2098574,-2.9220625,-4.8633283,1.22695\PG=C01 [X(C33H28N3)]\
```

S-1bA

```
1\1\GINC-LOCALHOST\FOpt\UB3LYP\def2SVP\C27H24N3(2)\PIOTR\24-Mar-2021\0
 \\#P UB3LYP/Def2SVP FOpt(tight) Geom=(NoDistance,NoAngle) fcheck\\naphthalene-1-(3-tBu-benzoTriazin-1-yl)-8-Ph opt in vac\\0,2\N,-0.26317277
59,-0.8640481569,-0.6847128834\N,-2.5997748409,0.5737328331,-0.8229142
361\C,-2.4695825804,-0.5578829578,-0.1247260552\N,-1.3668824891,-1.292
8257606,-0.0167343628\C,0.856682456,2.1337400688,-2.5852277776\C,0.929
7008971,0.914153555,-1.913364575\C,-0.2327639051,0.3590617826,-1.35297
16209\C,-1.4769784322,1.056271611,-1.4310962966\C,-1.5150561122,2.2852
723713,-2.1274225966\C,-0.3664156094,2.8154795638,-2.7014687465\H,-2.4
770669122,2.798411499,-2.1804533099\H,-0.4109847408,3.768617766,-3.233
9785418\H,1.7638954897,2.5594529455,-3.0207730612\H,1.8826768402,0.393
3612715,-1.8257148871\C,0.9319127993,-1.609570572,-0.4060437072\C,1.68
2974274,-2.2849852604,-1.4296443805\C,1.3536980654,-1.6082010421,0.912
6344592\C,1.273725713,-2.4556749248,-2.8032368461\C,2.9662287527,-2.81
84536735,-1.0317519742\C,2.5658707559,-2.2173688299,1.2949526471\H,0.7
329467101,-1.1005079594,1.6523955852\C,2.1797122622,-2.9938815483,-3.7
097205846\C,3.836013634,-3.3816046044,-2.0059951398\C,3.3692662041,-2.
7830788927,0.3314915775\H,2.8745891233,-2.2014276681,2.342667014\C,3.4
64476116,-3.4380867022,-3.3281832844\H,1.8594995451,-3.1232421138,-4.7
460311256\H,4.8056121368,-3.7663180527,-1.6796919264\H,4.3366106749,-3
.2164577025,0.5980857042\H,4.1365241542,-3.8610458532,-4.0787705994\C,
-0.103999984,-2.1933038261,-3.3215985595\C,-1.2104981285,-2.8869706015
,-2.8006528093\C,-0.3029200619,-1.3506694726,-4.4297166481\C,-2.476403
4655,-2.7391793122,-3.3710357754\H,-1.0749840877,-3.5529514203,-1.9458
275126\C,-1.5715653838,-1.1963461356,-4.9944398755\H,0.5458787963,-0.8
003690683,-4.8424075306\C,-2.6630382831,-1.8921002433,-4.4680353686\H,
-3.3222433819,-3.294994827,-2.9584313832\H,-1.7067466206,-0.5272654019
,-5.8480813917\H,-3.6559017515,-1.7750112447,-4.9094507708\C,-3.706014
1215,-1.0432197679,0.6462191867\C,-3.4638244466,-2.4034704887,1.317742
5541\C,-4.0337269659,0.0158704708,1.7230402792\C,-4.8895946741,-1.1518
052052,-0.3379609098\H,-3.2176907866,-3.1798548794,0.5781652789\H,-2.6
308667785,-2.3604369779,2.0339184571\H,-4.3711207958,-2.7170786408,1.8
58814816\H,-4.1958338496,1.0017823409,1.2634598686\H,-4.944592886,-0.2
687279654,2.2747274072\H,-3.2117568675,0.1079440787,2.4518777401\H,-5.
8074066593,-1.437675683,0.2011972985\H,-5.0621385439,-0.1935833571,-0.
8476291434\H,-4.6948624681,-1.916036824,-1.1071401461\\Version=ES64L-G
09RevD.01\State=2-A\HF=-1206.6960057\S2=0.765122\S2-1=0.\S2A=0.750145\
RMSD=5.240e-09\RMSF=7.322e-07\Di pole=1.1431731,-0.1474806,-0.2662631\Q
uadrupole=3.3129541,-4.4013141,1.08836,-1.1791148,1.9081413,-2.7590704
\PG=C01 [X(C27H24N3)]\\
```

R-1bA

```
1\1\GINC-LOCALHOST\FOpt\UB3LYP\def2SVP\C27H24N3(2)\PIOTR\24-Mar-2021\0
 \\#P UB3LYP/Def2SVP FOpt(tight) Geom=(NoDistance,NoAngle) fcheck\\naphthalene-1-(3-tBu-benzoTriazin-1-yl)-8-Ph opt in vac\\0,2\N,0.743186327
4,1.5307766481,-0.5587825749\N,3.4367982174,1.253267972,-0.0967673734\
C,2.8560212465,2.4175492617,-0.4002839117\N,1.5625657831,2.6126789274,
-0.638289164\C,1.0286843371,-2.1636042793,-0.2083361523\C,0.4482177599
,-0.9174277042,-0.4412023283\C,1.238006308,0.2418761615,-0.3654403677\
C,2.6370933389,0.1469853566,-0.0937254439\C,3.1890334487,-1.1315690213
,0.1459082071\C,2.3964280707,-2.2713901292,0.0948276842\H,4.2587566302
,-1.180871111,0.3576878208\H,2.8383665947,-3.2536044579,0.2791403038\H
,0.4087910146,-3.0615437643,-0.2666771146\H,-0.6126354715,-0.843067953
4,-0.6781226695\C,-0.6092561164,1.7727309529,-0.9759778463\C,-1.738844
```

7442, 1.5612676181, -0.1114853529\c, -0.7746674973, 2.1849598098, -2.287283
 5923\c, -1.67770255, 1.2556210764, 1.29784596\c, -3.0416597858, 1.650354337
 3, -0.7314735846\c, -2.0575754697, 2.3564277332, -2.8452815899\h, 0.1178763
 045, 2.3533554257, -2.8917171821\c, -2.8525770812, 0.9236405754, 1.96241353
 23\c, -4.208253882, 1.3229813136, 0.013308305\c, -3.1674311361, 2.062503752
 6, -2.0866261585\h, -2.1590424963, 2.6826219822, -3.8828596855\c, -4.113943
 0409, 0.9332691628, 1.3280862977\h, -2.7970033919, 0.6981074457, 3.02977299
 \h, -5.179601066, 1.3868962072, -0.4836816\h, -4.1701815247, 2.1399970551, -
 2.5145648461\h, -5.0088563376, 0.6715192954, 1.8977718815\c, -0.449182311,
 1.3687581131, 2.1425970675\c, 0.2171942034, 2.5993913577, 2.2781688048\c, -
 0.0159023505, 0.2828618043, 2.9240208983\c, 1.2851071686, 2.7366395323, 3.1
 672247136\h, -0.1098579797, 3.4570723835, 1.686526729\c, 1.0584705693, 0.41
 84669481, 3.8069273176\h, -0.5197988313, -0.6815291199, 2.8258263936\c, 1.7
 118122537, 1.6471594341, 3.933213824\h, 1.783685759, 3.7042315783, 3.266235
 5972\h, 1.3869819979, -0.4413128079, 4.3964236786\h, 2.5508500798, 1.756485
 4464, 4.6248776249\c, 3.7747126371, 3.6435647083, -0.5078101624\c, 2.979227
 5081, 4.9346067855, -0.7533616728\c, 4.5826116586, 3.770708495, 0.800774594
 1\c, 4.7459962953, 3.4008466052, -1.685228281\h, 2.3972257892, 4.8823249843
 , -1.6845534657\h, 2.2694643526, 5.1321669368, 0.0636675853\h, 3.6712644819
 , 5.7892413547, -0.8239317698\h, 5.1392878799, 2.8458422472, 1.006821445\h,
 5.2973302391, 4.6064587004, 0.7266749162\h, 3.91838591, 3.9660599365, 1.657
 65831\h, 5.457279597, 4.2383251212, -1.7731921402\h, 5.3151131983, 2.471703
 7002, -1.5358469528\h, 4.1999729334, 3.3192004147, -2.6394340588\\Version=
 ES64L-G09RevD.01\State=2-A\HF=-1206.6960057\S2=0.765122\S2-1=0.\S2A=0.
 750145\RMSD=5.155e-09\RMSF=7.386e-07\DIPOLE=-1.085578,-0.4578361,-0.10
 67894\Quadrupole=1.4266966,-1.5679419,0.1412453,1.2988195,4.1127601,-2
 .7479019\PG=C01 [X(C27H24N3)]\\

16. References

- (1) Fulmer, G. R.; Miller, A. J. M.; Sherden, N. H.; Gottlieb, H. E.; Nudelman, A.; Stoltz, B. M.; Bercaw, J. E.; Goldberg, K. I. NMR chemical shifts of trace impurities: Common laboratory solvents, organics, and gases in deuterated solvents relevant to the organometallic chemist, *Organometallics* **2010**, *29*, 2176-2179.
- (2) Constantinides, C. P.; Obijalska, E.; Kaszyński, P. Access to 1,4-dihydrobenzo[e][1,2,4]triazin-4-yl derivatives, *Org. Lett.* **2016**, *18*, 916-919.
- (3) Zhou, Y.; Zhang, Z.; Jiang, Y.; Pan, X.; Ma, D. Synthesis of 1,2,4-benzotriazines via copper(I) iodide/1H-pyrrole-2-carboxylic acid catalyzed coupling of o-haloacetanilides and N-Boc hydrazine, *Synlett* **2015**, 1586-1590.
- (4) Berezin, A. A.; Zissimou, G.; Constantinides, C. P.; Beldjoudi, Y.; Rawson, J. M.; Koutentis, P. A. Route to benzo- and pyrido-fused 1,2,4-triazinyl radicals via N'-(het)aryl-N'-[2-nitro(het)aryl]hydrazides, *J. Org. Chem.* **2014**, *79*, 314-327.
- (5) Dominguez, Z.; Lopez-Rodriguez, R.; Alvarez, E.; Abbate, S.; Longhi, G.; Pischel, U.; Ros, A. Azabora[5]helicene charge-transfer dyes show efficient and spectrally variable circularly polarized luminescence, *Chem. Eur. J.* **2018**, *24*, 12660-12668.

- (6) Romero-Nieto, C.; López-Andarias, A.; Egler-Lucas, C.; Gebert, F.; Neus, J.-P.; Pilgram, O. Paving the way to novel phosphorus-based architectures: A noncatalyzed protocol to access six-membered heterocycles, *Angew. Chem. Int. Ed.* **2015**, *54*, 15872-15875.
- (7) PK, Rigaku Oxford Diffraction Ltd, Yarnton, Oxfordshire, England, 2018.
- (8) Sheldrick, G. M. *SHELXT – Integrated space-group and crystal- structure determination*, *Acta Cryst., Sect. A* **2015**, *A71*, 3-8.
- (9) Sheldrick, G. M. Crystal structure refinement with *SHELXL*, *Acta Cryst., Sect. C* **2015**, *C71*, 3-8.
- (10) Neugebauer, F. A.; Rimmmer, G. ENDOR and triple resonance studies of 1,4-dihydro-1,2,4-benzotriazinyl radicals and 1,4-dihydro-1,2,4-benzotriazine radical cations, *Magn. Reson. Chem* **1988**, *26*, 595-600.
- (11) Hande, A. A.; Darrigan, C.; Bartos, P.; Baylère, P.; Pietrzak, A.; Kaszyński, P.; Chrostowska, A. UV-Photoelectron spectroscopy of stable radicals: The electronic structure of planar Blatter radicals as materials for organic electronics, *Phys. Chem. Chem. Phys.* **2020**, *22*, 23637–23644.
- (12) Connelly, N. G.; Geiger, W. E. Chemical redox agents for organometallic chemistry, *Chem. Rev.* **1996**, *96*, 877-910.
- (13) Reist, M.; Testa, B.; Carrupt, P.-A.; Jung, M.; Schurig, V. Racemization, enantiomerization, diastereomerization, and epimerization: Their meaning and pharmacological significance, *Chirality* **1995**, *7*, 396-400.
- (14) Gaussian 09, Revision A.02, M. J. Frisch, G. W. Trucks, H. B. Schlegel, G. E. Scuseria, M. A. Robb, J. R. Cheeseman, G. Scalmani, V. Barone, B. Mennucci, G. A. Petersson, H. Nakatsuji, M. Caricato, X. Li, H. P. Hratchian, A. F. Izmaylov, J. Bloino, G. Zheng, J. L. Sonnenberg, M. Hada, M. Ehara, K. Toyota, R. Fukuda, J. Hasegawa, M. Ishida, T. Nakajima, Y. Honda, O. Kitao, H. Nakai, T. Vreven, J. A. Montgomery, Jr., J. E. Peralta, F. Ogliaro, M. Bearpark, J. J. Heyd, E. Brothers, K. N. Kudin, V. N. Staroverov, R. Kobayashi, J. Normand, K. Raghavachari, A. Rendell, J. C. Burant, S. S. Iyengar, J. Tomasi, M. Cossi, N. Rega, J. M. Millam, M. Klene, J. E. Knox, J. B. Cross, V. Bakken, C. Adamo, J. Jaramillo, R. Gomperts, R. E. Stratmann, O. Yazyev, A. J. Austin, R. Cammi, C. Pomelli, J. W. Ochterski, R. L. Martin, K. Morokuma, V. G. Zakrzewski, G. A. Voth, P. Salvador, J. J. Dannenberg, S. Dapprich, A. D. Daniels, O. Farkas, J. B. Foresman, J. V. Ortiz, J. Cioslowski, and D. J. Fox, Gaussian, Inc., Wallingford CT, 2009.